# Supporting Information

# Robust interaction of cobalt phthalocyanine and nitrogen doped ordered mesoporous carbon for $CO_2$ reduction paired with electro-oxidative synthesis of sulfonamide derivatives

*Samin Barat Abtahi*[a], *Faranak Jafari Hafshejani*[a], *Fahimeh Varmaghani*[*ab], *Babak Karimi*[*ab] *and Hamzeh H. Veisi*[a]

[a] Department of Chemistry, Institute for Advanced Studies in Basic Sciences (IASBS), Zanjan 45137-66731, Iran

[b] Research Center for Basic Sciences and Modern Technologies (RBST), Institute for Advanced Studies in Basic Sciences (IASBS), Zanjan 45137-66731, Iran

## Contents

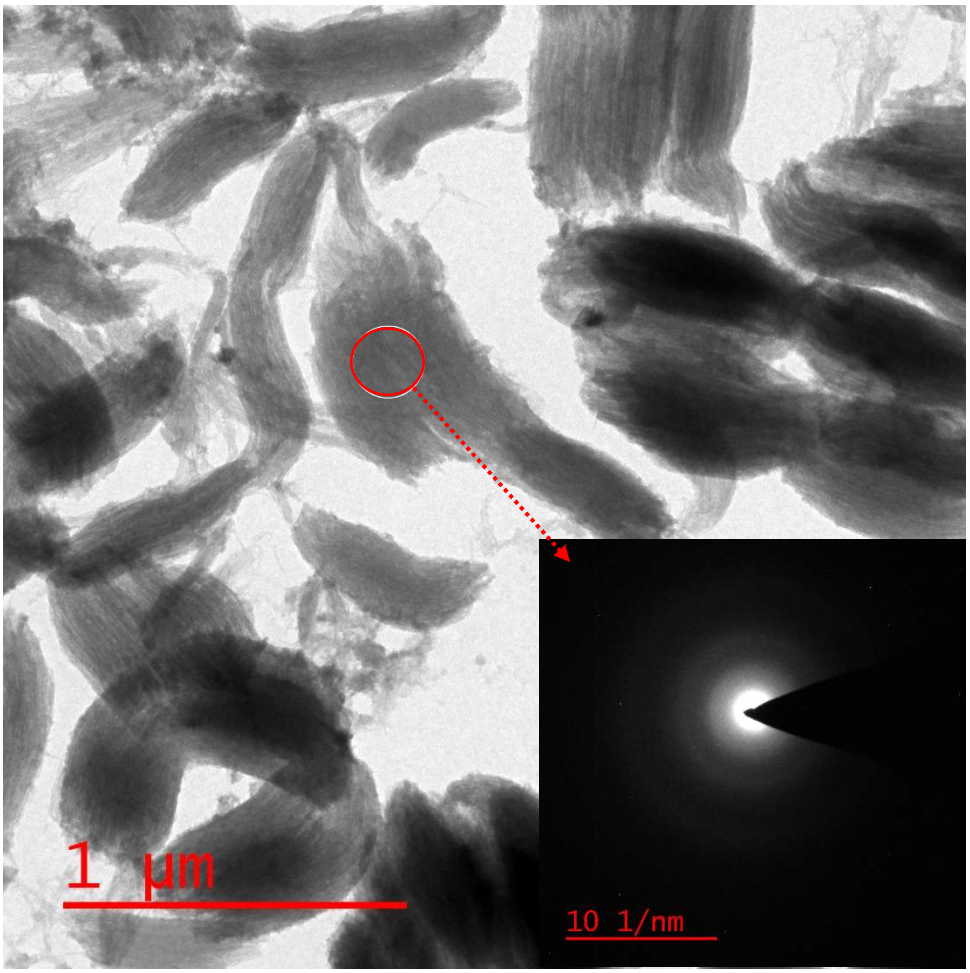
1 µm
10 1/nm

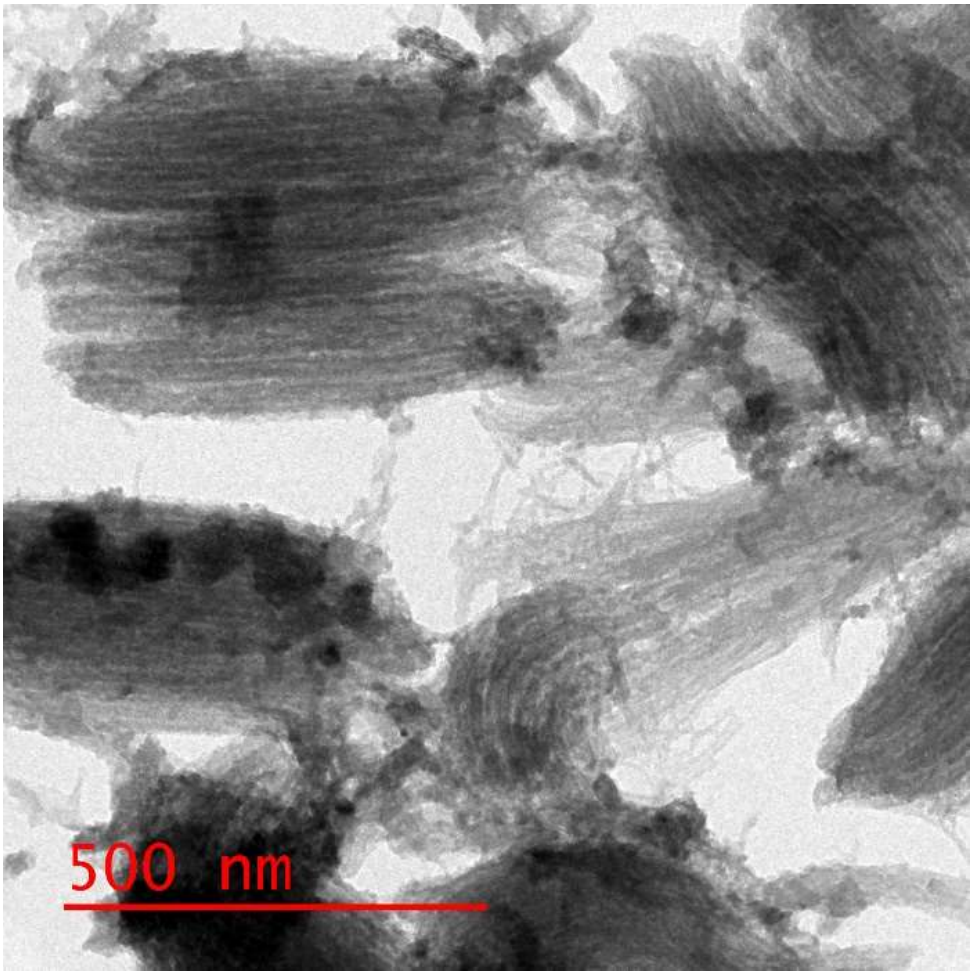
500 nm

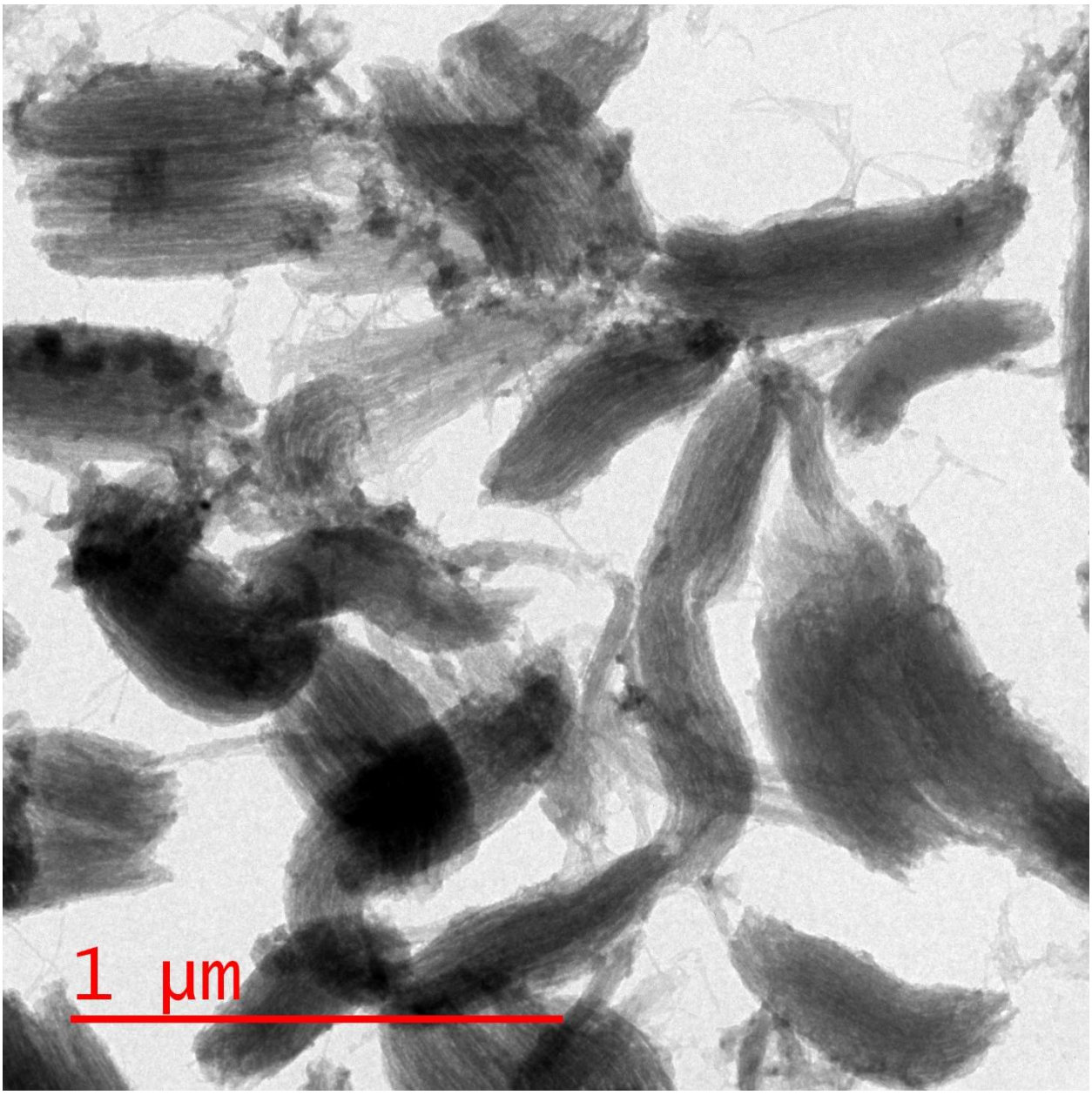
1 µm

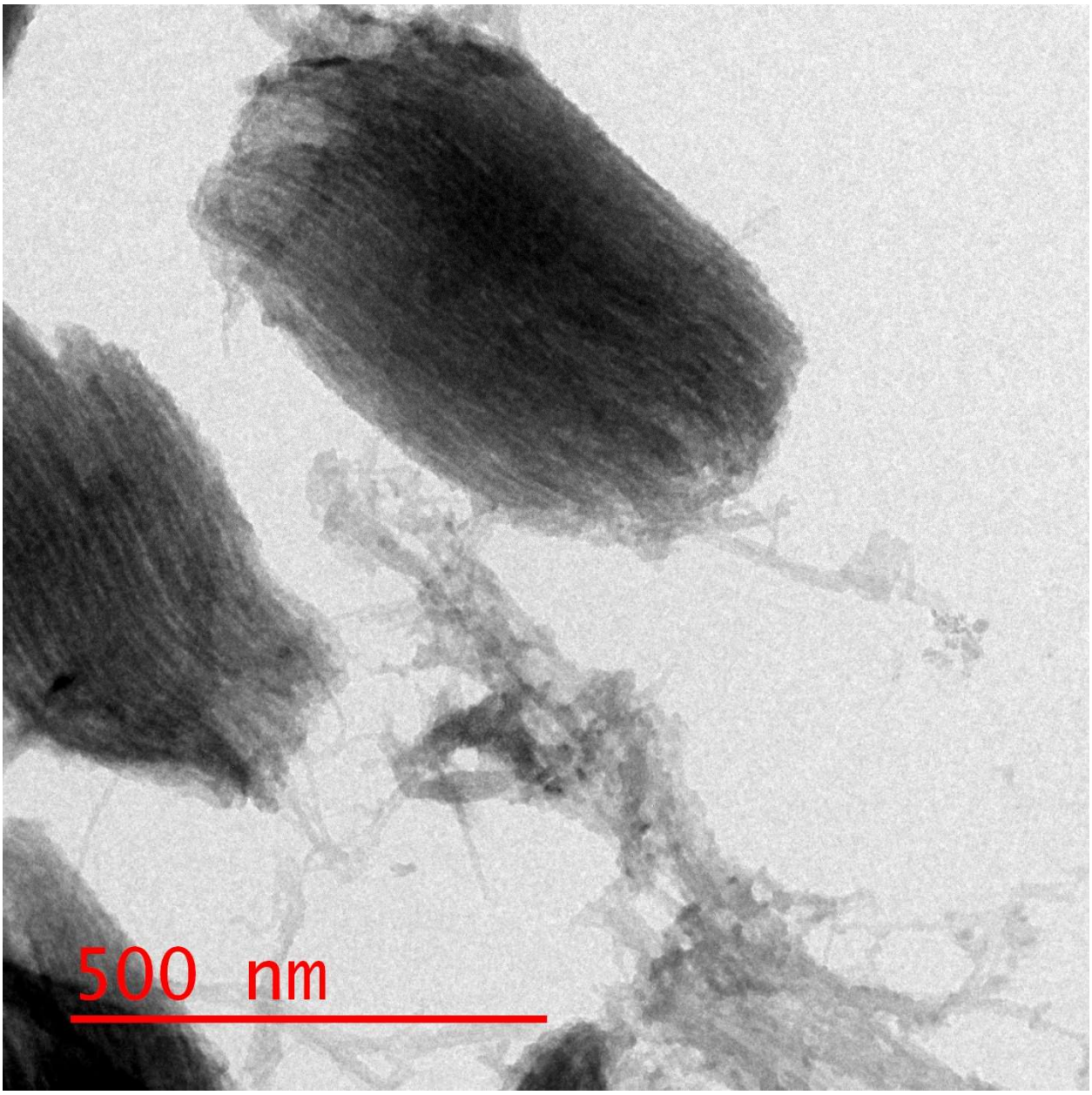
500 nm

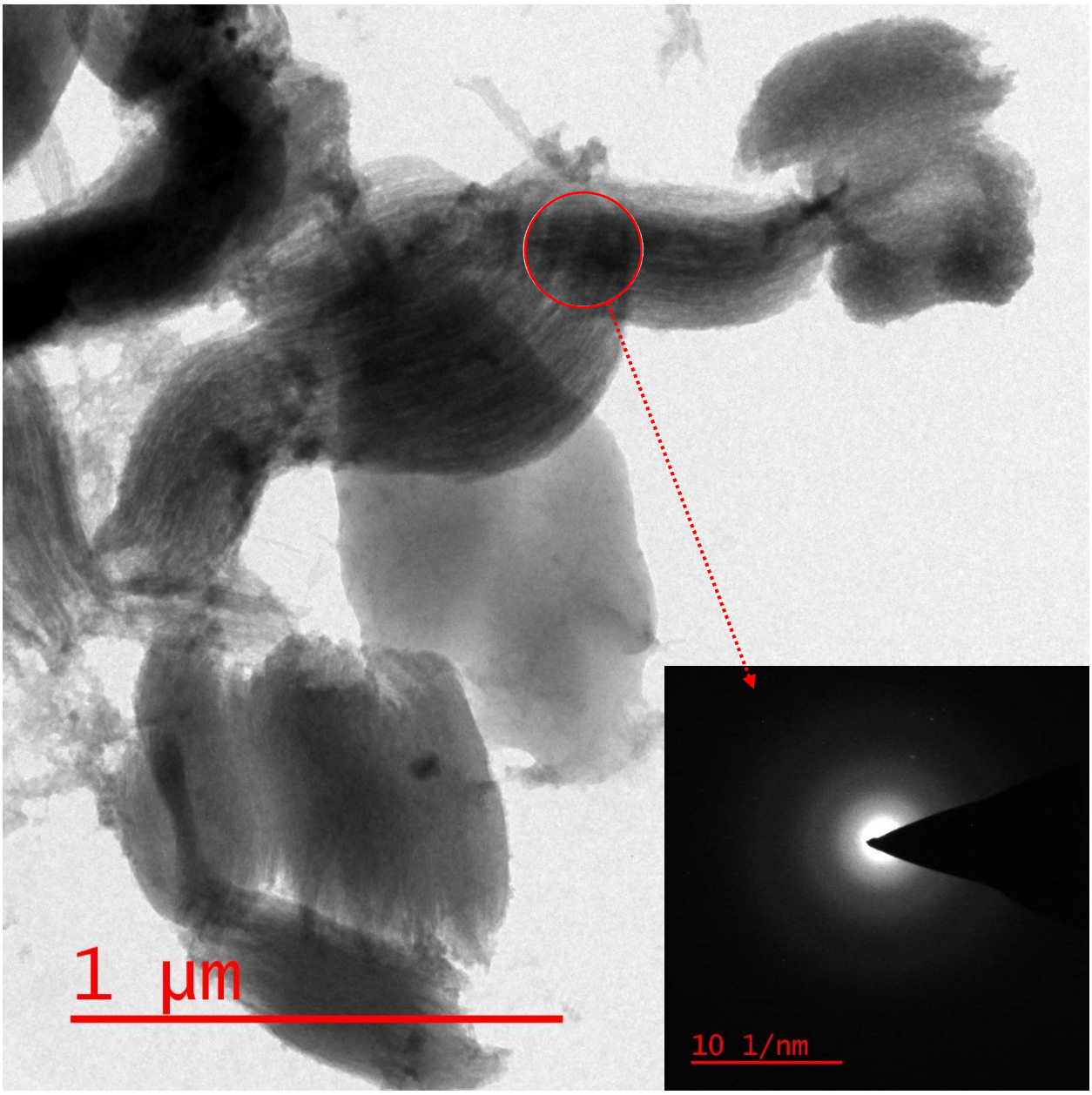
1 µm
10 1/nm

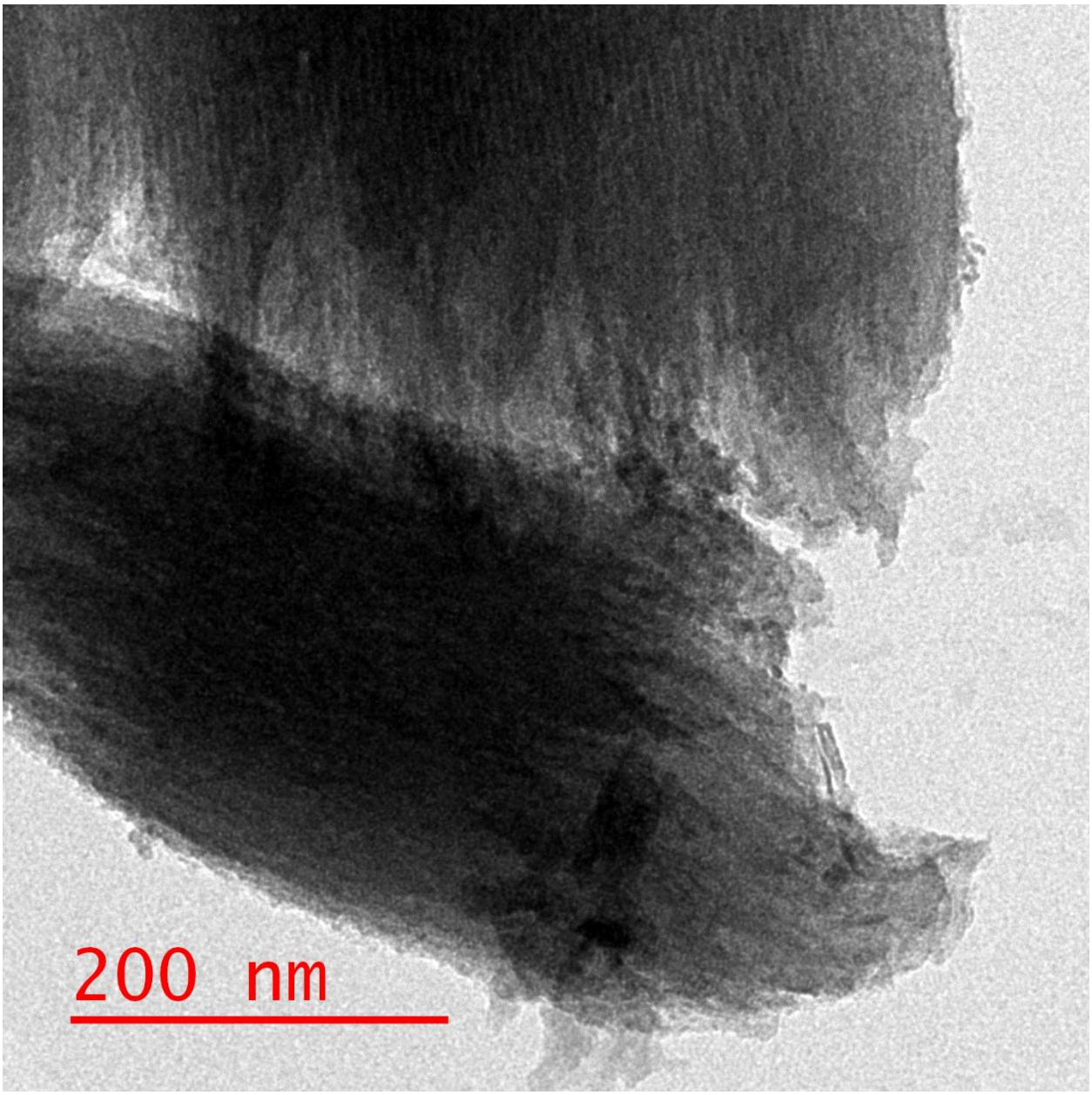
200 nm

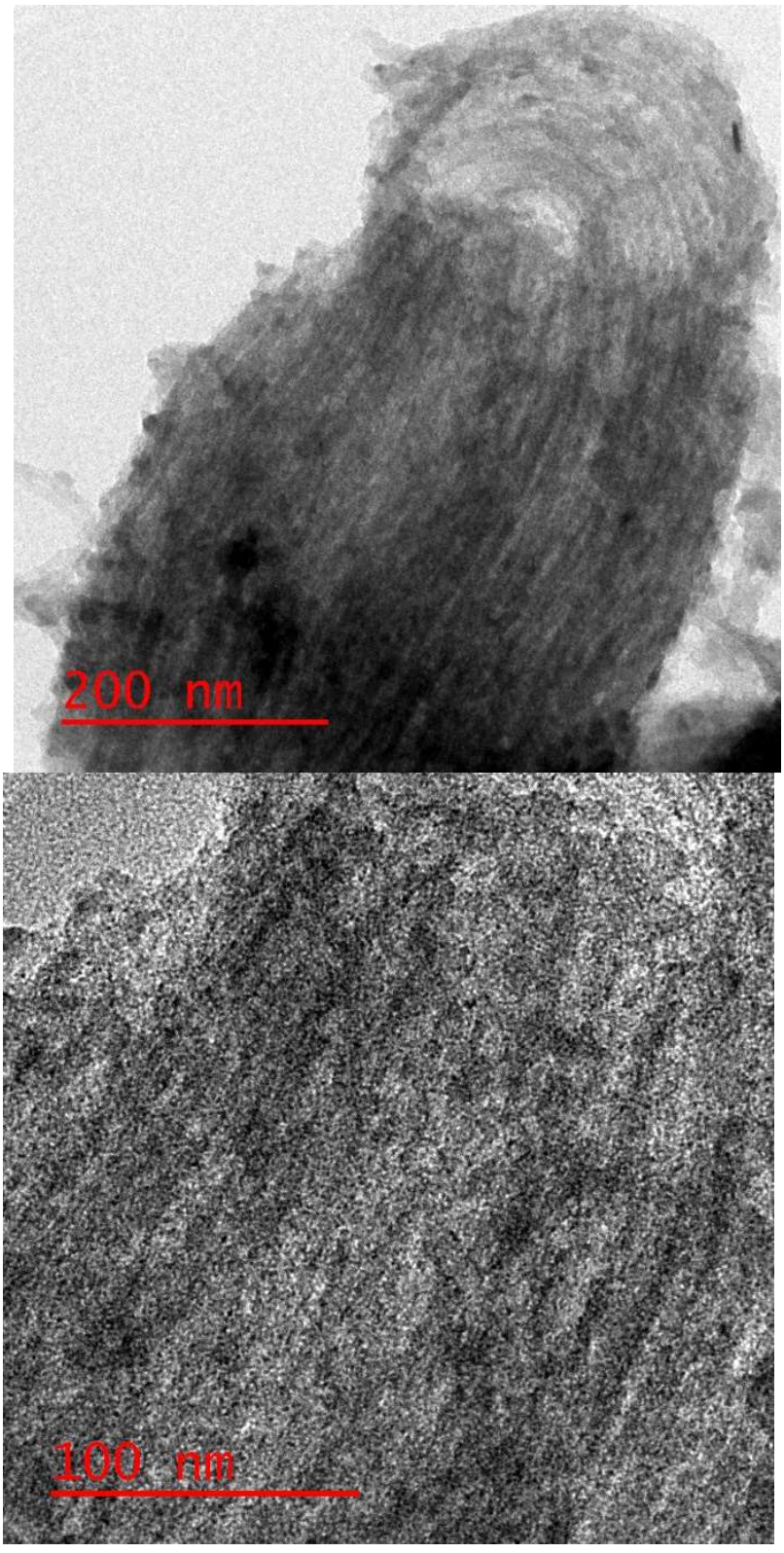


**Figure S1**: TEM images and SAED patterns of CoPc@GIOMC (0.9%)

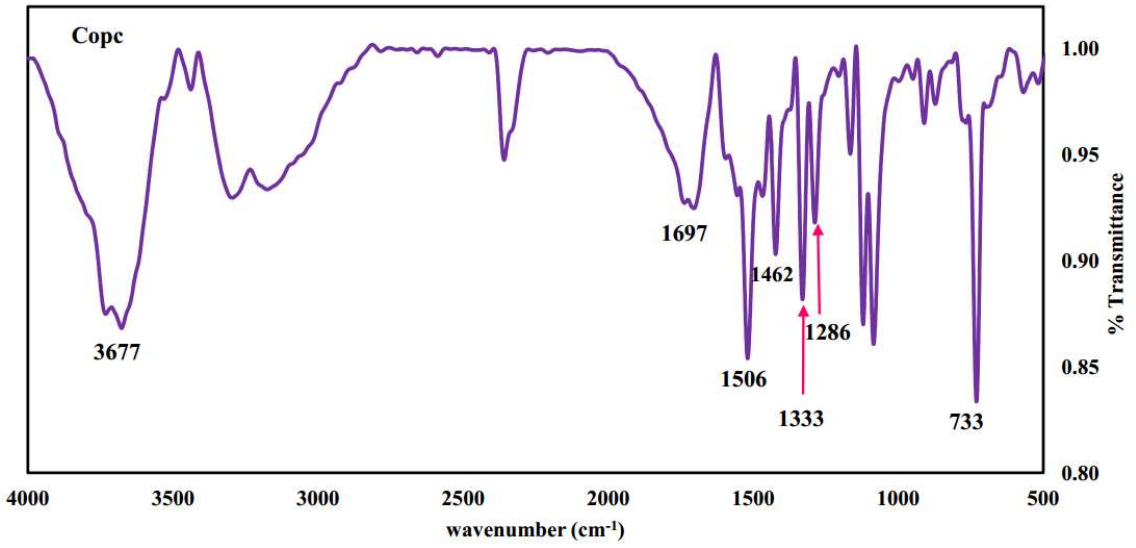


**Figure S2**: FTIR spectra of CoPc

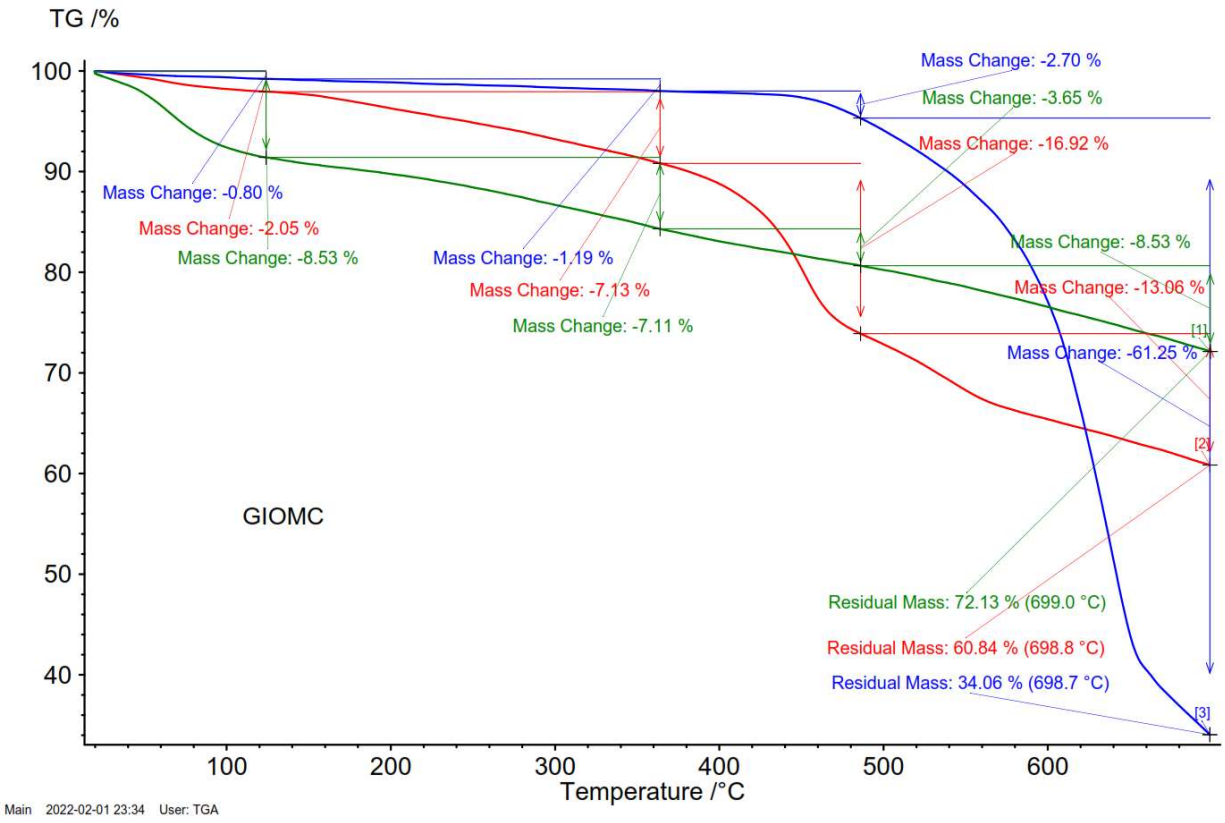


**Figure S3:** TGA analysis of CoPc: blue, CoPc@GIOMC: red and GIOMC: green

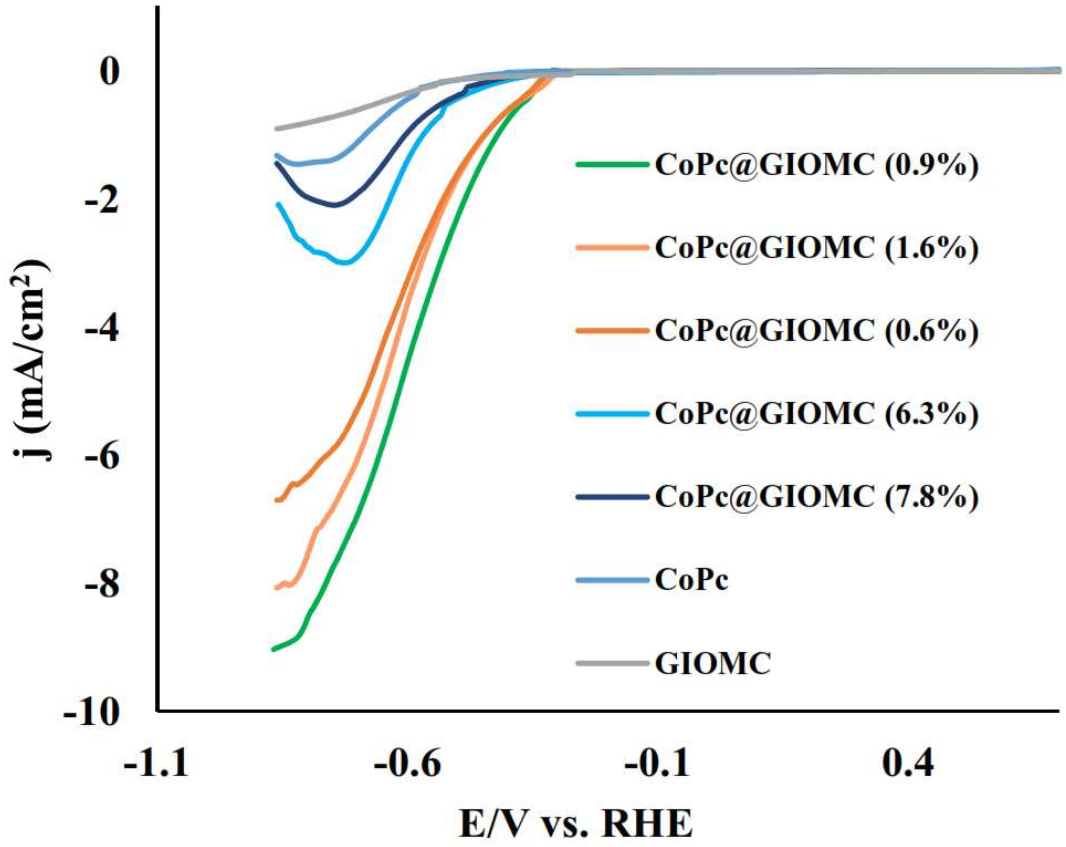


**Figure S4:** LSVs of the GC electrode modified with CoPc, GIOMC and CoPc@GIOMC with various Co loading in 0.5 $KHCO_3$. Scan rate: 5 $mVs^{-1}$

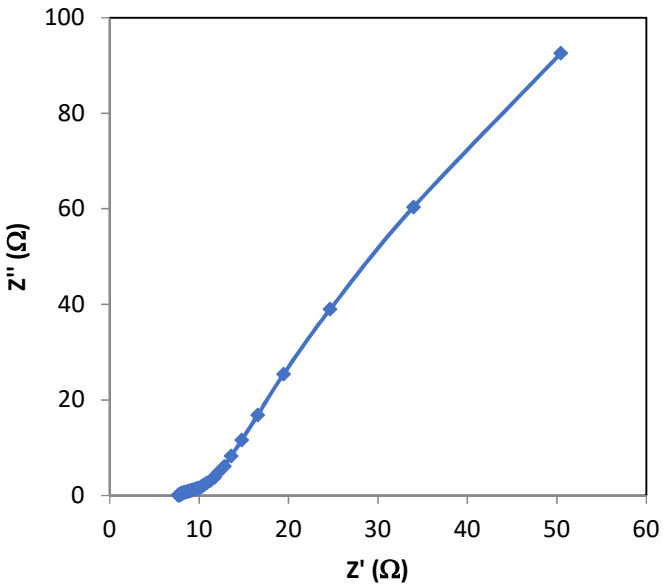


**Figure S5:** Nyquist plots for CoPc@GIOMC (0.9%) in 0.5 $KHCO_3$

PHA was prepared through chemical reduction of NB using a mixture of ammonium chloride and zinc powder as reducing agent and catalyst, respectively. Figure S6I, curve a, demonstrates cyclic voltammetry of NB before the reaction. The voltammogram was recorded in the potential range of -0.7 to +0.8 V vs. RHE, by transferring 1 ml of the reaction solution to the voltammetric cell followed by adding 9 ml aqueous phosphate buffer solution (pH=2). An irreversible cathodic signal ($C_0$) at -0.3 V vs. RHE appeared upon sweeping the potential toward negative direction, which is well-matched with the electrochemical reduction potential of NB to PHA (Ref. 47 of the paper). A redox couple appeared during the reverse and second scan ($A_1/C_1$), which is attributed to the redox process of the electrogenerated PHA to nitrosobenzene via two-electron, two-proton dependent electron transfer. The voltammogram of the solution at the end of the reaction was again recorded in the same conditions as curve a in Figure S6I (curve b). The negligible $C_0$ peak accompanied by significant increase of $A_1/C_1$ redox couple demonstrates the synthesis of PHA in high yields. It is important to note that the chemical reduction of NT, did not proceed well, giving low yields of the corresponding products. The voltammogram of the solution at the end of the reaction (Figure S7) showed incomplete reduction by displaying $C_0$ cathodic peak with significant height, possibly due to electron donating effect of the methyl group. This observation shows that the highly efficient reduction of NT can be only achieved by electro-reductive synthesis. In the next stage, THA was electrochemically synthesized in a divided cell containing NT, 20 ml ethanol and 60 ml aqueous phosphate buffer solution (optimal pH value of 3, 0.5 M) by applying the controlled-potential electrolysis at -0.4 V vs. RHE. Figure S6II displays the cyclic voltammograms during the electro-reduction. The gradual decrease of the cathodic peak heights ($C_0$) indicates successful conversion of NT to THA. Encouraged by these results, the same procedure was then

employed for the electroreduction of NBCl to HABCl under otherwise the same electrochemical conditions.

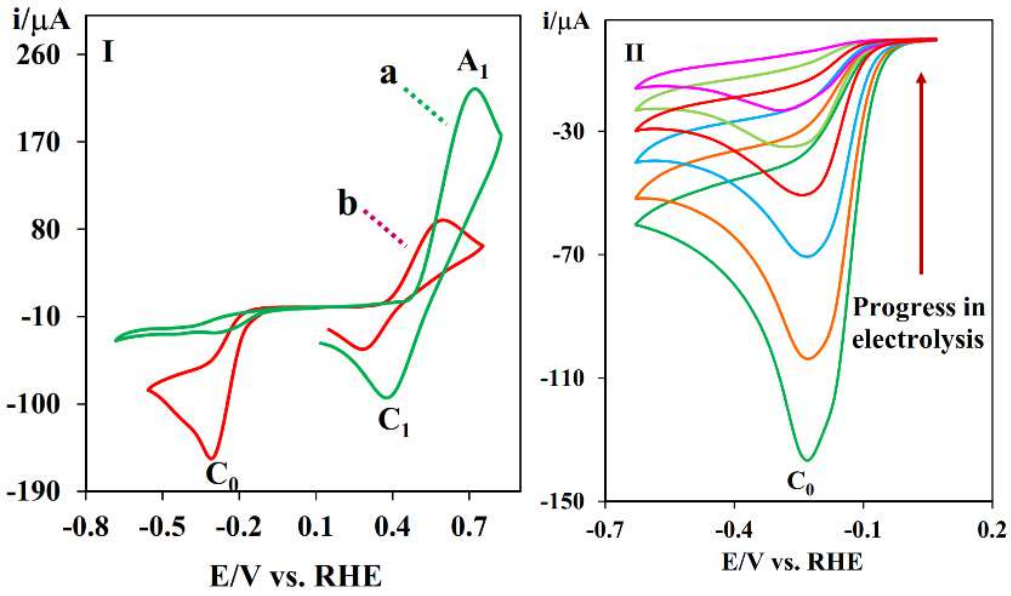


Figure S6. (I) cyclic voltammograms of (a) nitrobenzene at the start and (b) at the end of chemical reduction at GCE at 100 mV/s in phosphate buffer solution (pH=2), (II) cyclic voltammograms of 0.5 mmol 4-nitrotoluene in phosphate buffer solution (pH=3) at GCE during electrolysis at -0.32 V vs. RHE.

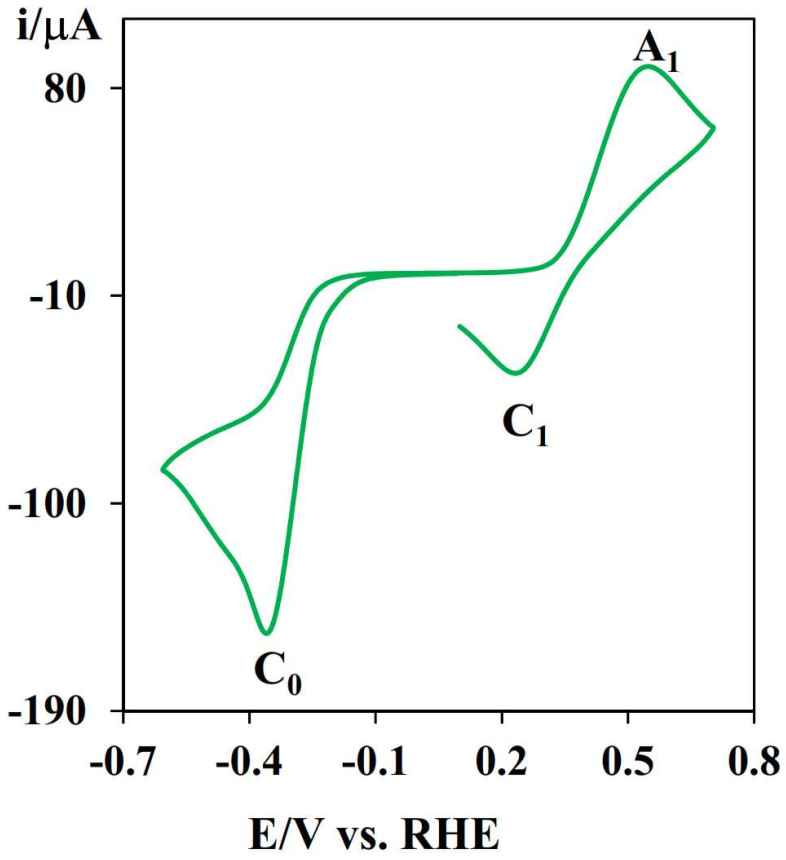


**Figure S7:** cyclic voltammogram of the solution of chemical reduction of 4-nitrotoluene at the end of chemical reduction at GCE at 100 mV/s in phosphate buffer solution (pH=2).

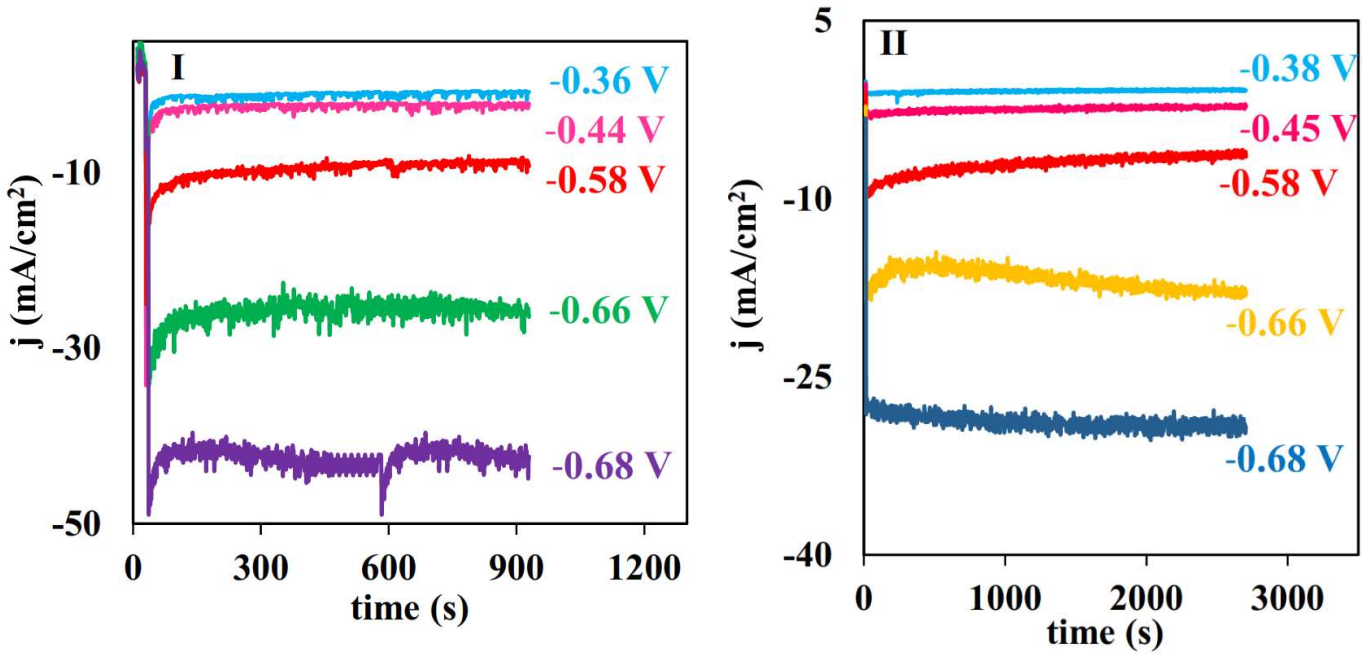


**Figure S8:** Chronoamperograms of the cathodic part of the paired electrolysis of $eCO_2RR$ coupled with electrochemical oxidation of (I) THA and (II) catechol in the presence of TSA at different potentials.

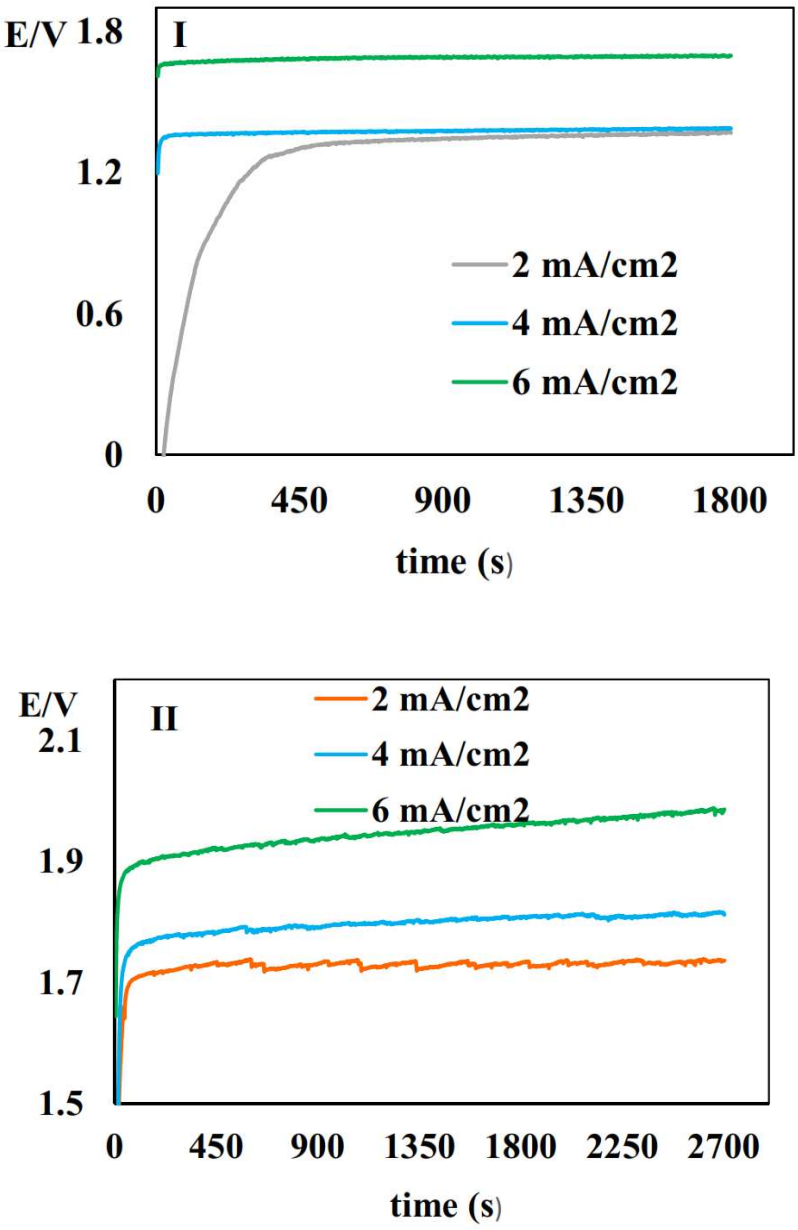


**Figure S9:** E-t plot of two-electrode setup of the paired electrolysis of $eCO_2RR$ coupled with electrochemical oxidation of (I) PHA and (II) catechol in the presence of TSA at various current density

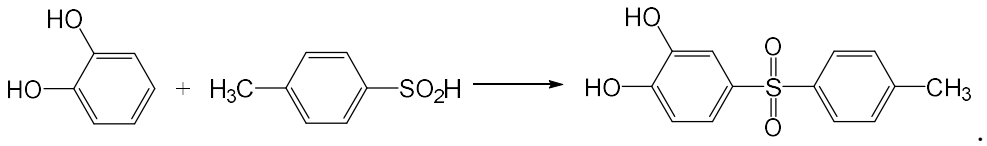


**Figure S10:** Anodic reaction of oxidation of catechol in the presence of TSA in the eCO2RR electrolyzer

The internal standard method was used to plot the calibration curve. Anisole was used as internal standard. The calibration curve was plotted in concentration range of 0.4 to 1.4 M catechol, where the concentration of the analyzed samples was in that range. Fig. S8 shows GC chromatogram of the standard for the ratio of catechol/anisole of 1.38.

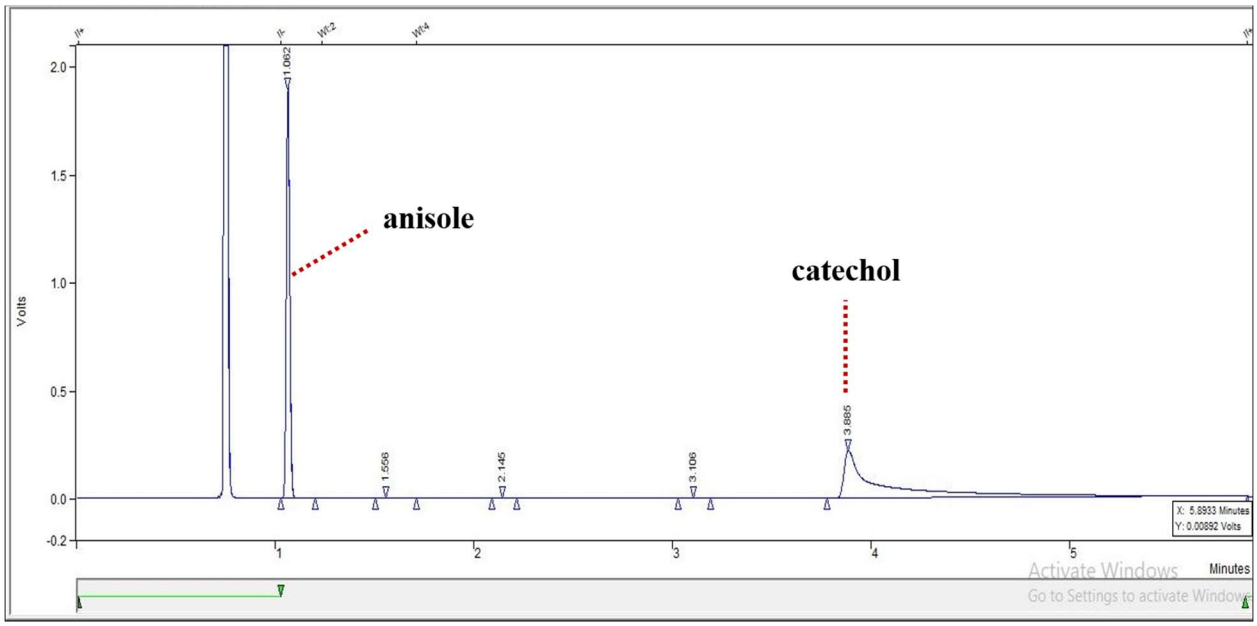


| Peak No. | Peak Name | Result () | Ret. Time (min) | Time Offset (min) | Area (counts) | Sep. Code | Width 1/2 (sec) | Status Codes |
|---|---|---|---|---|---|---|---|---|
| 1 | | 41.8925 | 1.062 | 0.000 | 2157956 | BB | 1.1 | |
| 2 | | 0.2146 | 1.556 | 0.000 | 11055 | BB | 3.1 | |
| 3 | | 0.0234 | 2.145 | 0.000 | 1203 | BB | 2.6 | |
| 4 | | 0.0303 | 3.106 | 0.000 | 1561 | BB | 4.7 | |
| 5 | | 57.8392 | 3.885 | 0.000 | 2979399 | BB | 4.5 | |
| | Totals: | 100.0000 | | 0.000 | 5151174 | | | |

**Figure S11:** Chromatogram of the standard sample for plotting the calibration curve using the internal standard method for the ratio of catechol/anisole of 1.38.

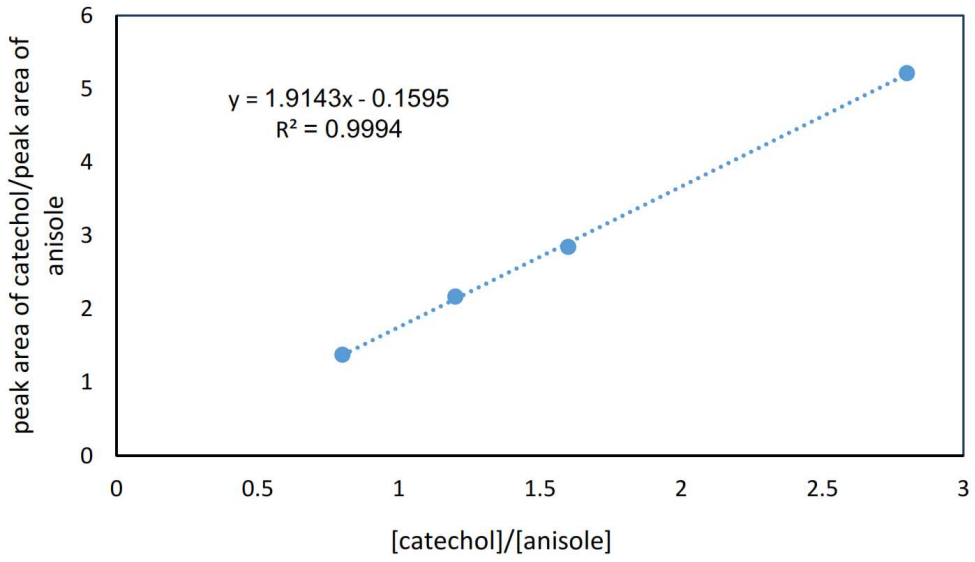


**Figure S12:** The plotting of calibration curve for determination of catechol. It should be noted that the calibration curve was plotted in concentration range of 0.4 to 1.4 M catechol, because the concentration of the analyzed samples was in that range.

To record the chromatogram at the end of the electrolysis, the solution was completely evaporated. Then, to remove the salt used as an electrolyte, the solid was washed with acetone and immediately evaporated, and then the resulting solid was dissolved in ethyl acetate and was introduced to GC. Figure S9 presents the chromatograms of the species after 135 minutes of the electrolysis. It should be noted that the signals related to the TSA and the product do not appear in the time range.

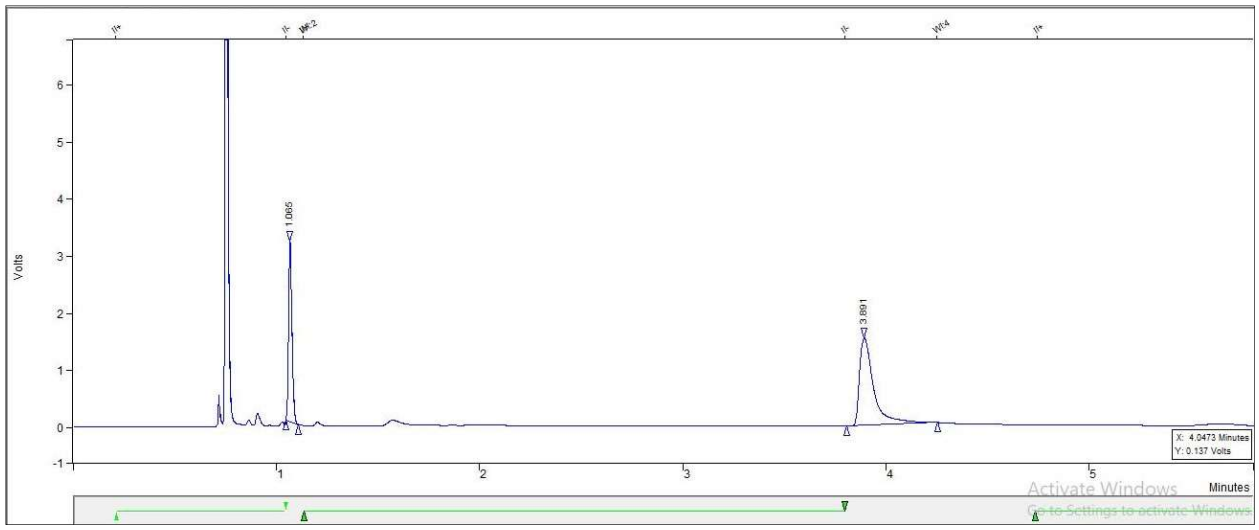


**Figure S13**. Chromatograms of the solution of the electrolysis cell after 135 minutes electrolysis at current density of 14 mA.

**Spectroscopic properties of 1-9**

*N*-Hydroxy-4-methyl-*N*-(*p*-tolyl)benzenesulfonamide (1). $^{1}$H NMR (400 MHz, DMSO-d6) δ = 2.28 (s, 3H, $CH_3$), 2.40 (s, 3H, $CH_3$), 6.96 (d, 2H, Ar-H), 7.11 (d, 2H, Ar-H), 7.32-7.38 (m, 4H, Ar-H), 11.00 (s, 1H, OH). $^{13}$C NMR (100 MHz, DMSO-d6) δ = 21.0, 21.6, 123.2, 129.2, 129.6, 129.7, 136.8, 140.7, 145.0 ppm. IR (KBr) ν = 3680, 3353, 2978, 2902, 1595, 1502, 1405, 1332, 1156, 1081, 814, 677 $cm^{-1}$. MS (EI) m/z (%) (relative intensity): 91 (46), 122 (100), 156 (3), 181 (3), 259 (5), 277 (10).

*N*-hydroxy-*N*-(*p*-tolyl)benzenesulfonamide (2). $^{1}$H NMR (400 MHz, DMSO-d6) δ = 2.28 (s, 3H, $CH_3$), 6.95 (d, 2H, Ar-H), 7.10 (d, 2H, Ar-H), 7.46 (d, 2H, Ar-H), 7.55-7.59 (t, 2H, Ar-H), 7.72-7.75 (t, 1H, Ar-H), 11.07 (s, 1H, OH). $^{13}$C NMR (100 MHz, DMSO-d6) δ = 21.0, 123.2, 129.2, 129.3, 129.7, 132.8, 134.5, 136.9, 140.6 ppm. IR(KBr), ν = 3679, 3361, 2979, 2901, 1504, 1403, 1250, 1162, 1086, 817, 686 $cm^{-1}$. MS (EI) m/z (%) (relative intensity): 91 (39), 106 (10), 122 (100), 142 (5), 167 (2), 180 (1), 247 (4), 263 (6).

4-Chloro-*N*-hydroxy-*N*-(*p*-tolyl)benzenesulfonamide (3). $^{1}$H NMR (400 MHz, DMSO-d6) δ = 2.29 (s, 3H, $CH_3$), 6.97 (d, 2H, Ar-H), 7.13 (d, 2H, Ar-H), 7.46 (d, 2H, Ar-H), 7.67 (d, 2H, Ar-H), 11.18 (s, 1H, OH). $^{13}$C NMR (100 MHz, DMSO-d6) δ = 21.1, 123.2, 129.4, 129.5, 131.5, 137.2, 139.6, 140.3 ppm. IR (KBr) ν = 3673, 3354, 2979, 2404, 1574, 1502, 1393, 1341, 1279, 1162, 1083, 705 $cm^{-1}$. MS (EI) m/z (%) (relative intensity): 91 (49), 106 (21), 122 (100), 159 (6), 176 (4), 281 (4), 297 (2).

4-((*N*-hydroxy-4-methylphenyl)sulfonamido)benzoyl chloride (4). $^{1}$H NMR (400 MHz, DMSO-d6) δ = 2.38 (s, 3H, CH3), 7.27 (d, 2H, Ar-H), 7.36 (s, 4H, Ar-H), 7.88 (d, 2H, Ar-H) ppm. $^{13}$C NMR (100 MHz, DMSO-d6) δ = 21.6, 122.1, 124.1, 129.1, 129.5, 129.9, 130.0, 130.1, 145.4,

147.0, 167.3. IR (KBr) ν =3336, 3112, 2850, 2671, 1688, 1526, 1426, 1346, 1156, 1093, 1015, 943, 806, 665.

4-(*N*-hydroxyphenylsulfonamido)benzoyl chloride (5). $^{1}$H NMR (400 MHz, DMSO-d6) δ = 7.28 (d, 1H, Ar-H), 7.47 (d, 1H, Ar-H), 7.66 (d, 1H, Ar-H), 7.91 (d, 1H, Ar-H), 8.14 (s, 4H, Ar-H), 8.20 (d, 1H, Ar-H), 8.40 (d, 1H, Ar-H), 11.44 (1H, OH), $^{13}$C NMR (100 MHz, DMSO-d6) δ = 122.3, 123.1, 124.2, 125.4, 124.5, 129.7, 130.2, 130.6, 130.9, 131.2, 131.3, 131.5, 131.8, 139.9, 146.6, 146.9, 166.7, 167.0, 167.2. IR (KBr) ν = 3438, 3300, 1690, 1601, 1504, 1455, 1287, 1166, 1090, 1015, 861, 726, 681.

*N*-hydroxy-4-methyl-*N*-phenylbenzenesulfonamide (6). $^{1}$H NMR (400 MHz, DMSO-d6) δ = 2.39 (s, 3H, $CH_3$), 7.10 (d, 2H, Ar-H), 7.23-7.27 (m, 1H, Ar-H), 7.29-7.37 (m, 6H, Ar-H), 11.08 (s, 1H, OH). $^{13}$C NMR (100 MHz, DMSO-d6) δ = 21.6, 123.1, 127.4, 128.8, 129.7, 130.0, 143.2, 145.1 ppm. IR (KBr) ν = 3374, 3074, 2925, 1596, 1486, 1353, 1183, 1162, 1090, 766, 694 $cm^{-1}$. MS (EI) m/z (%) (relative intensity): 91 (66), 107 (100), 139 (7), 155 (8), 182 (3), 247 (1), 263 (26).

*N*-Hydroxy-*N*-phenyl-benzenesulfonamide (7). $^{1}$H NMR (400 MHz, DMSO-d6) δ = 7.09 (d, 2H, Ar-H), 7.24-7.33 (m, 3H, Ar-H), 7.45 (d, 2H, Ar-H), 7.54-7.58 (t, 2H, Ar-H), 7.72-7.75 (t, 1H, Ar-H), 11.16 (s, 1H, OH). $^{13}$C NMR (100 MHz, DMSO-d6) δ = 123.1, 127.5, 128.8, 129.2, 129.6, 132.7, 143 ppm. IR (KBr), ν = 3375, 3068, 2857, 1593, 1485, 1447, 1346, 1171, 766, 685, 589 $cm^{-1}$. MS (EI) m/z (relative intensity): 107 (100), 125 (6), 142 (5), 167 (6), 233 (2), 249 (15).

4-Chloro-*N*-hydroxy-*N*-phenyl-benzenesulfonamide (8). $^{1}$H NMR (400 MHz, DMSO-d6) δ = 7.10 (d, 2H, Ar-H), 7.26-7.29 (m, 1H, Ar-H), 7.32-7.35 (m, 2H, Ar-H), 7.44 (d, 2H, Ar-H), 7.66 (d, 2H, Ar-H), 11.26 (s, 1H, OH). $^{13}$C NMR (100 MHz, DMSO-d6) δ = 123.1, 127.8, 129.0, 129.5, 131.5,

140.0, 142.7 ppm. IR (KBr) ν = 3356, 3094, 2850, 1577, 1487, 1350, 1175, 762, 567 $cm^{-1}$. MS (EI) m/z (relative intensity): 108 (100), 128 (3), 159 (6), 175 (4), 263 (3), 283 (9).

4-Tosylbenzene-1,2-diol (9). $^{1}H$ NMR (400 MHz, Acetone-d6) δ = 2.41 (s, 3H, $CH_3$), 7.00 (d, 1H, Ar-H), 7.37-7.42 (m, 4H, Ar-H), 7.81 (d, 2H, Ar-H), $^{13}C$ NMR (100 MHz, Acetone) δ = 20.1, 114.9, 115.5, 120.5, 127.2, 129.8, 133.1, 140.3, 143.7, 145.5, 150.0, 208.1.

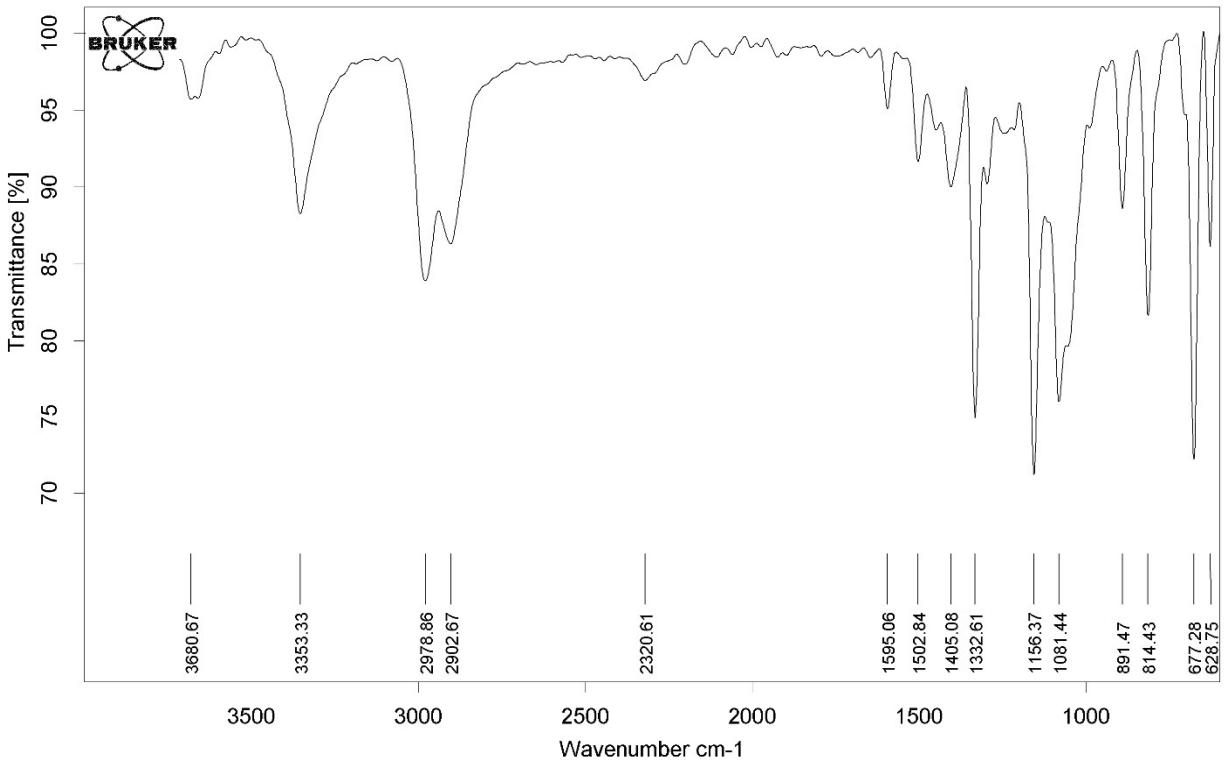


**Figure S14**. FTIR spectra of 1

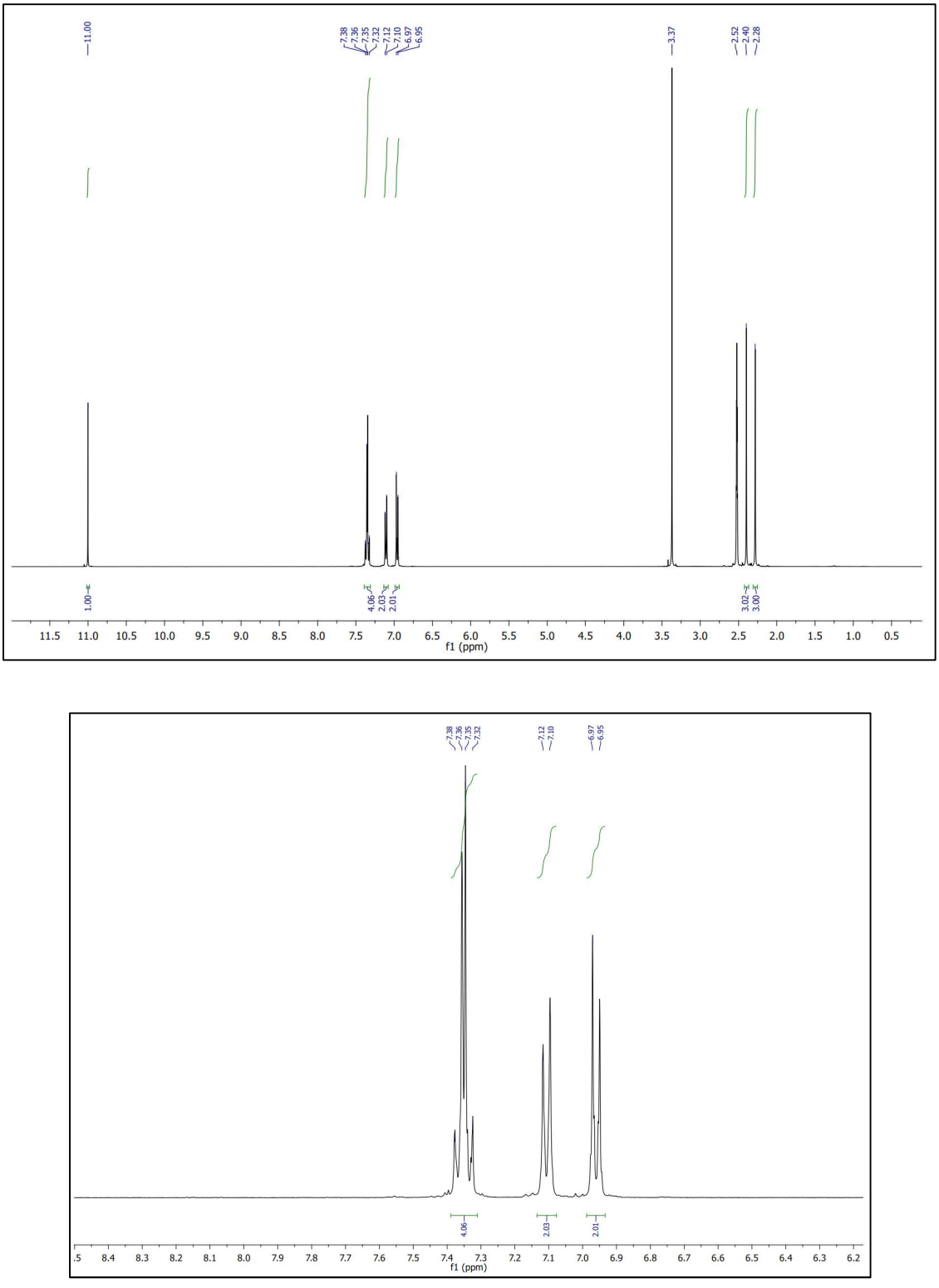


**Figure S15**. [1]HNMR spectra of 1

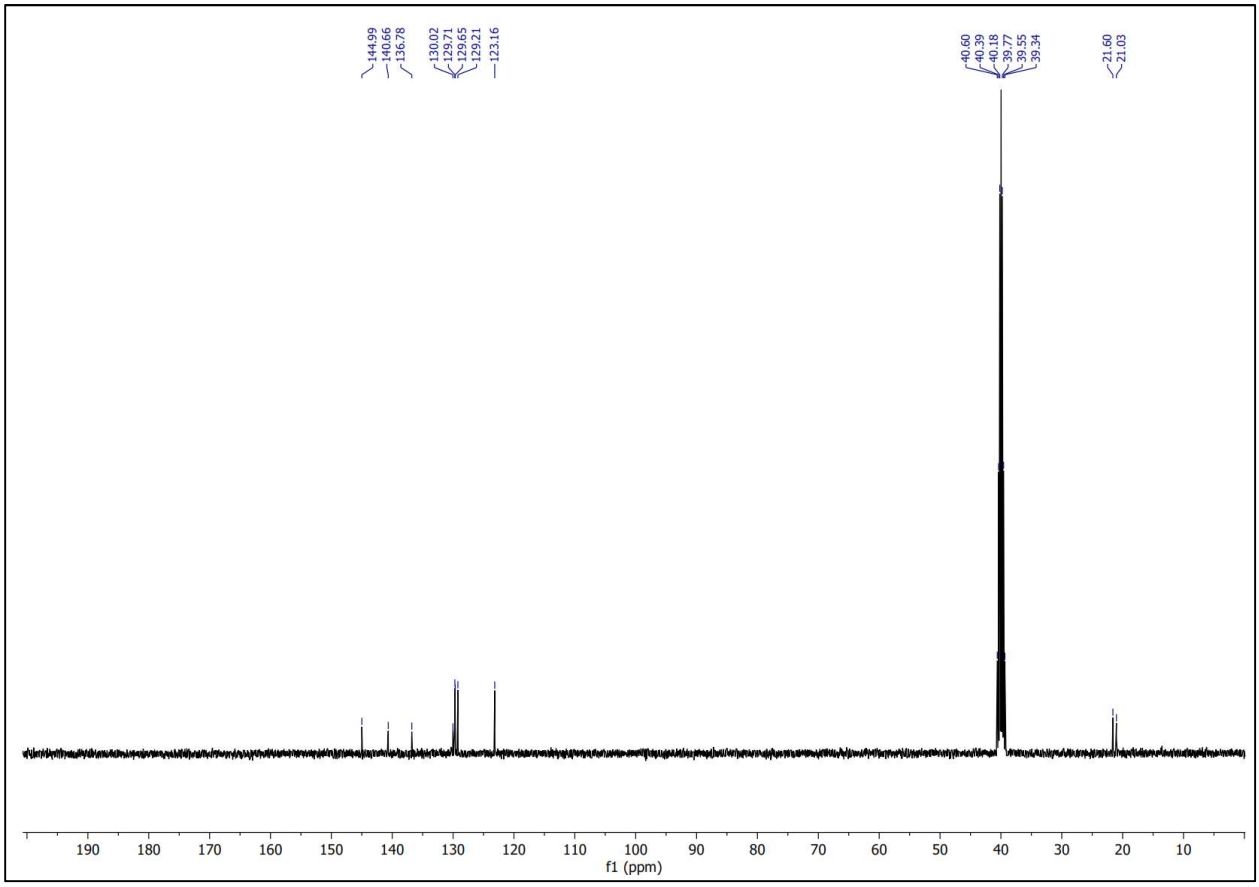


**Figure S16**. $^{13}$CNMR spectra of 1

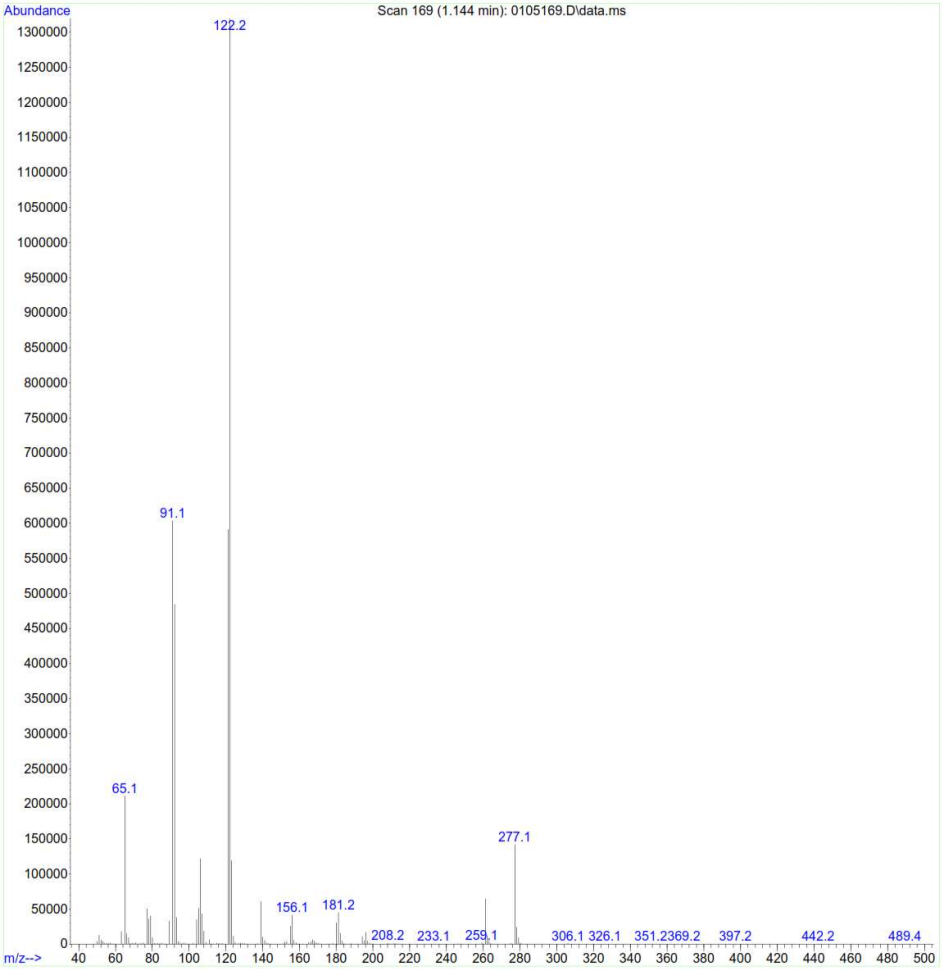


**Figure S17**. MS spectra of 1

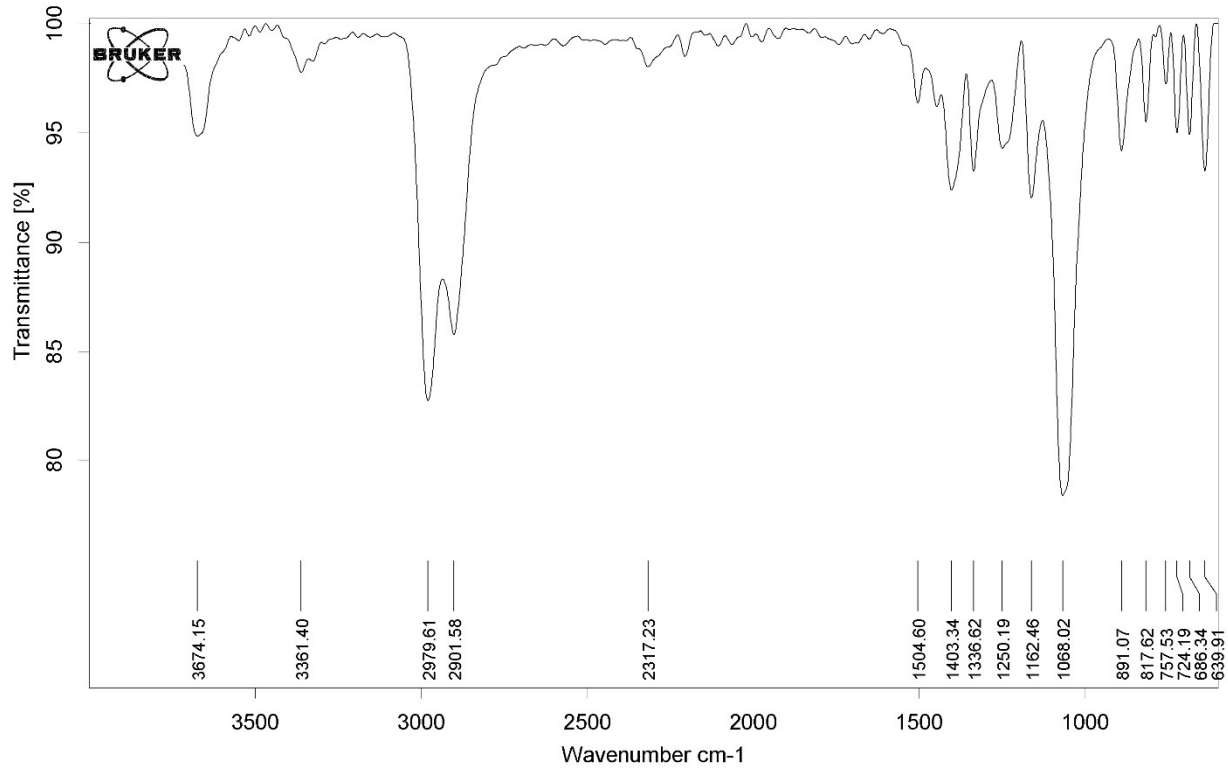


**Figure S18**. FTIR spectra of 2

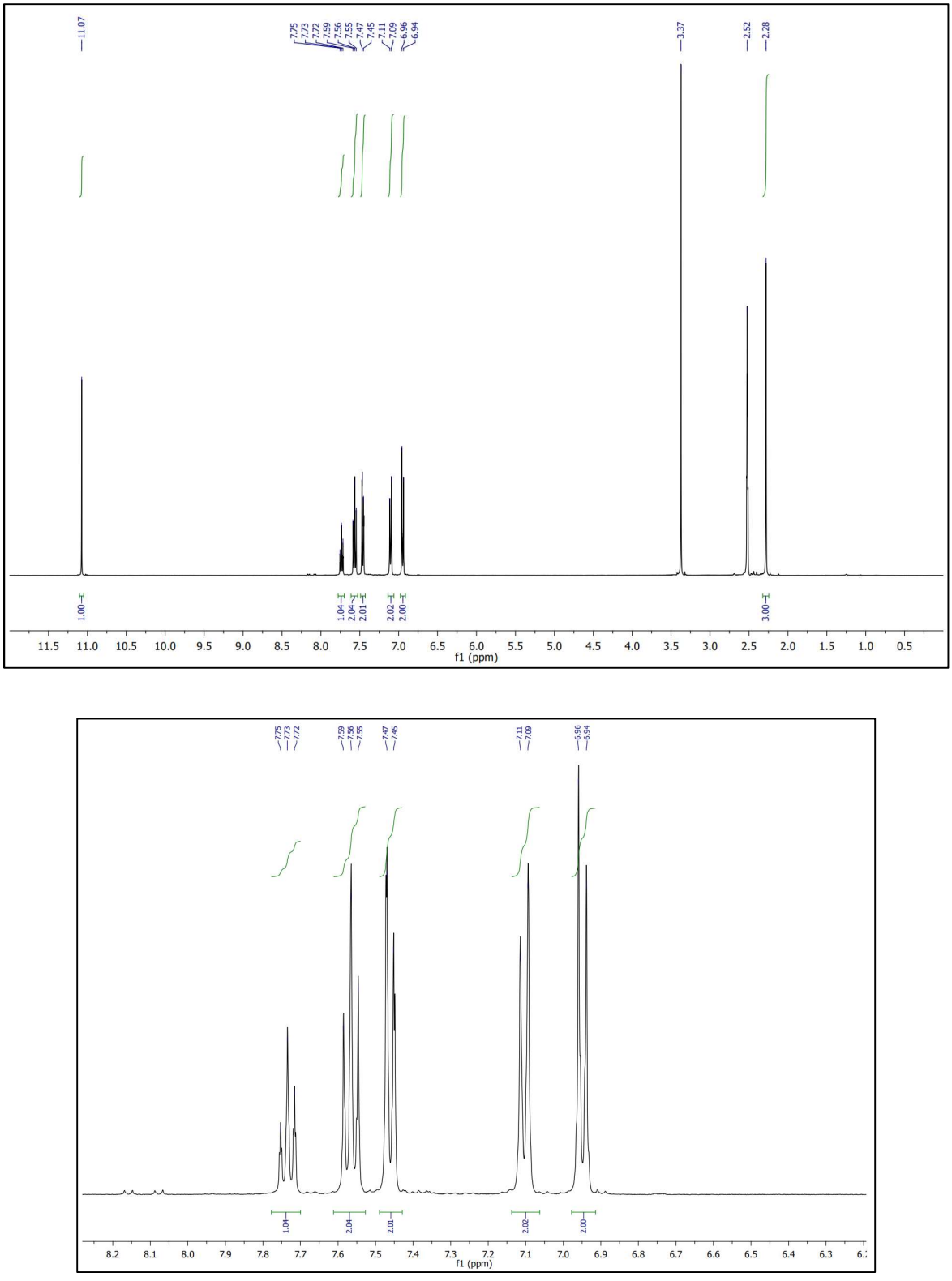


**Figure S19**. [1]HNMR spectra of 2

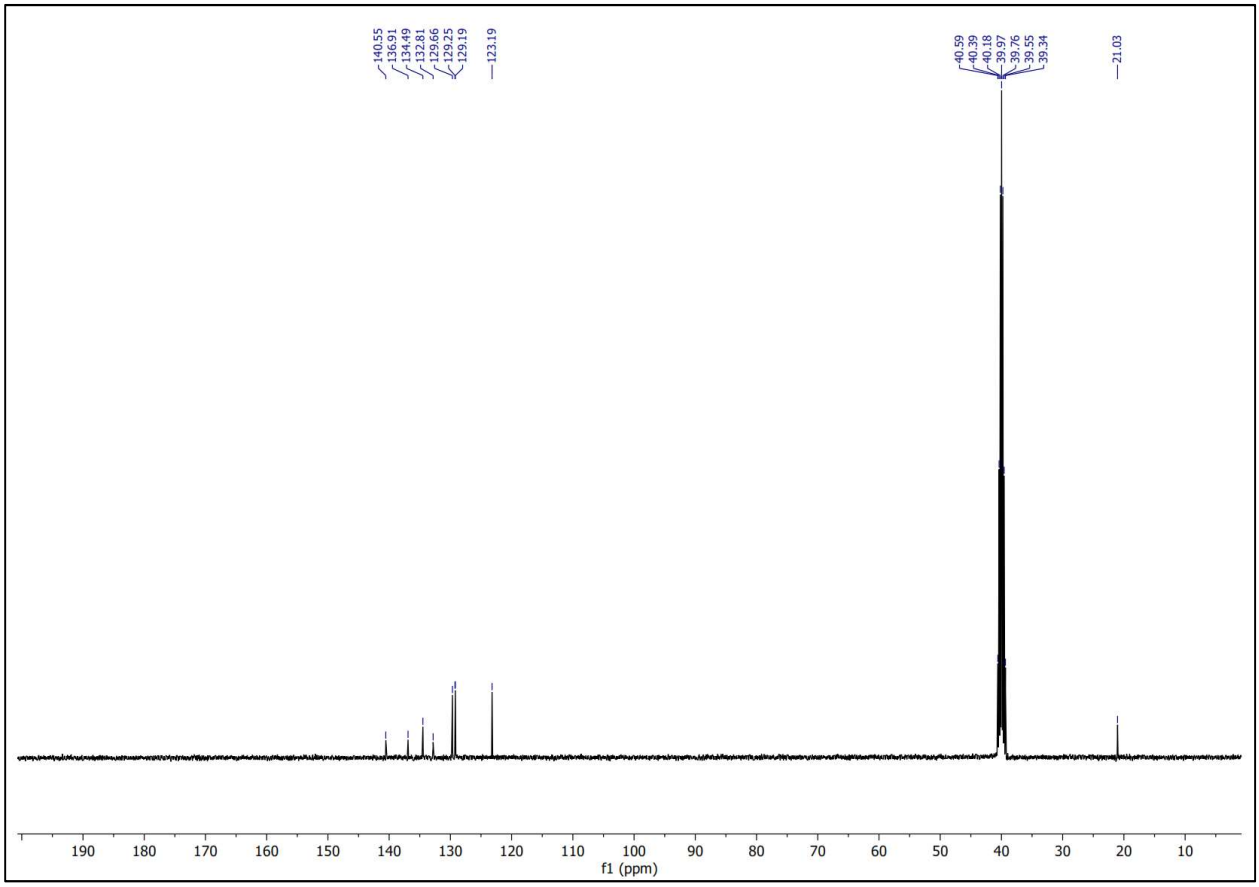


**Figure S20**. $^{13}$CNMR spectra of 2

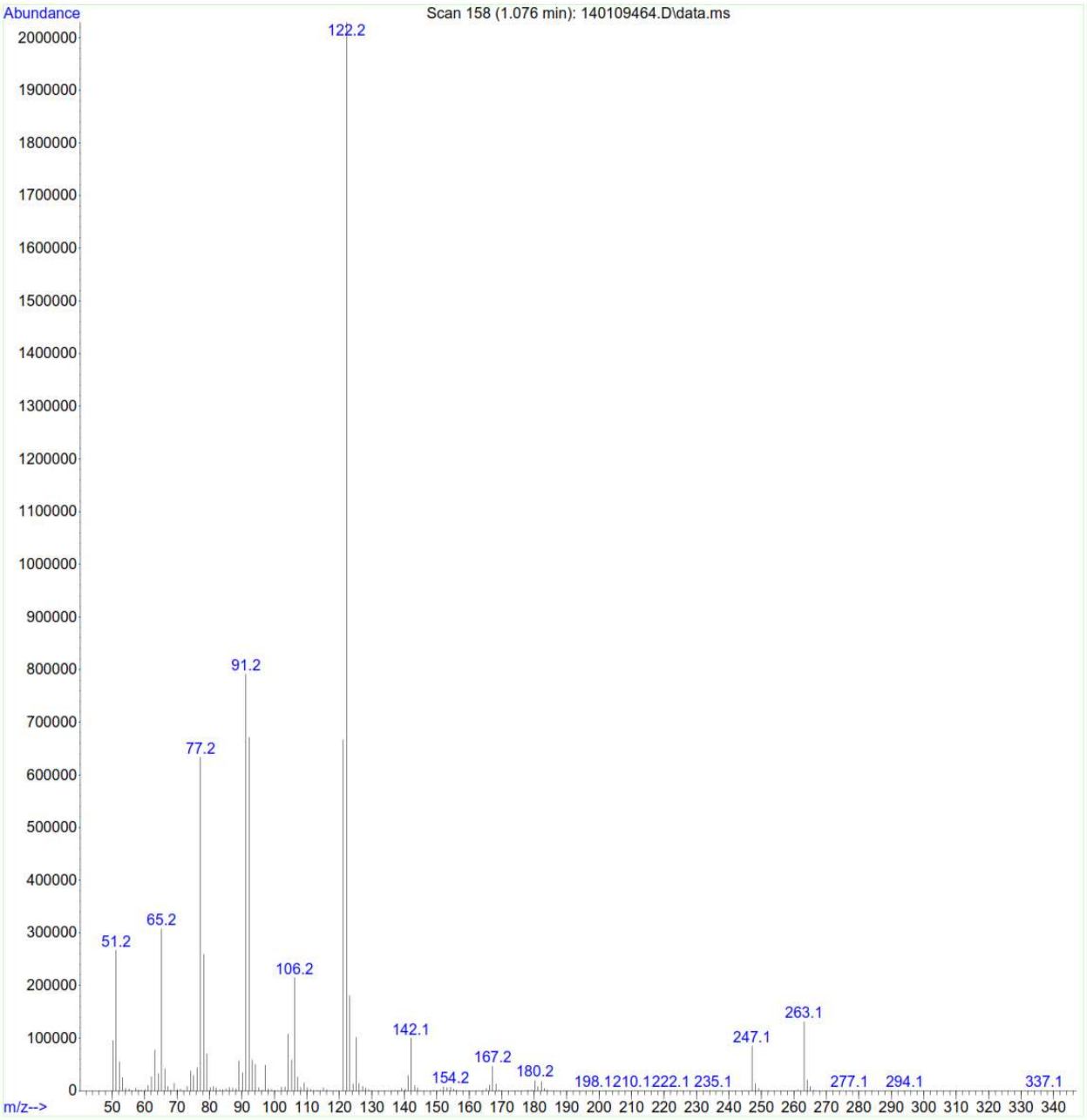


**Figure S21**. MS spectra of 2

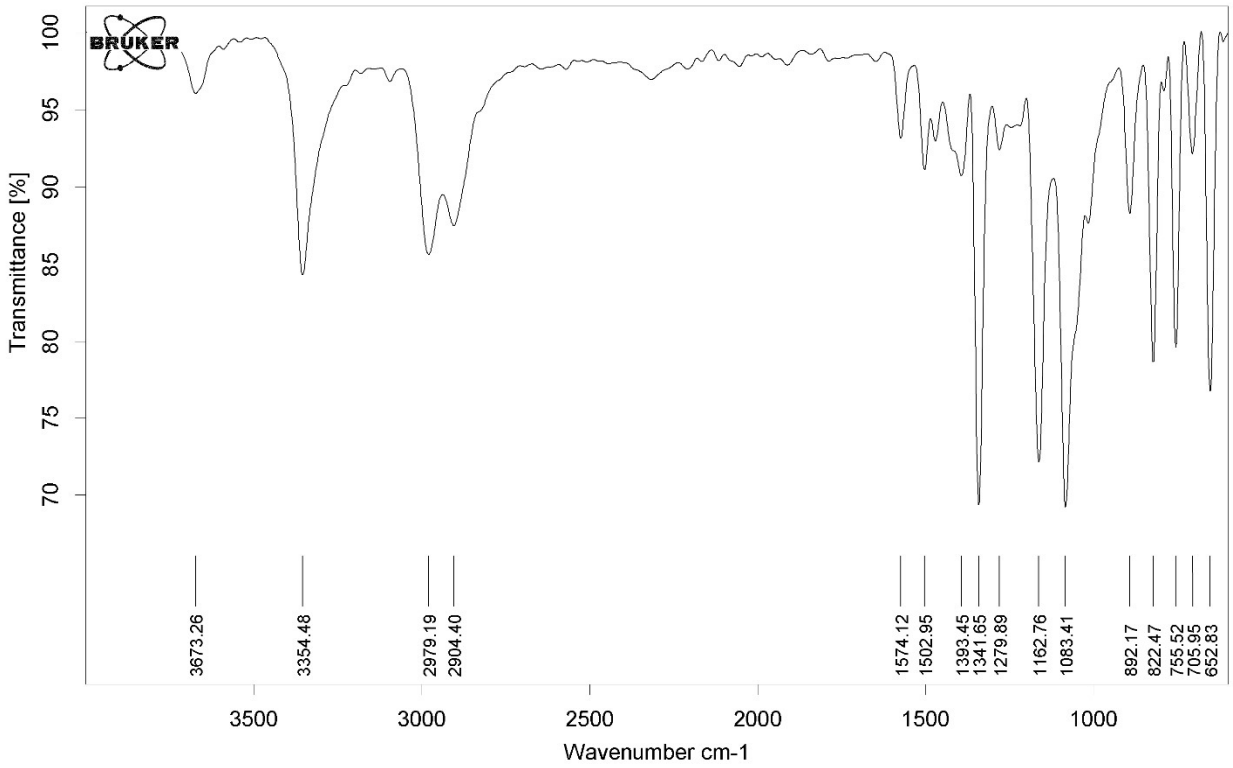


**Figure S22**. FTIR spectra of 3

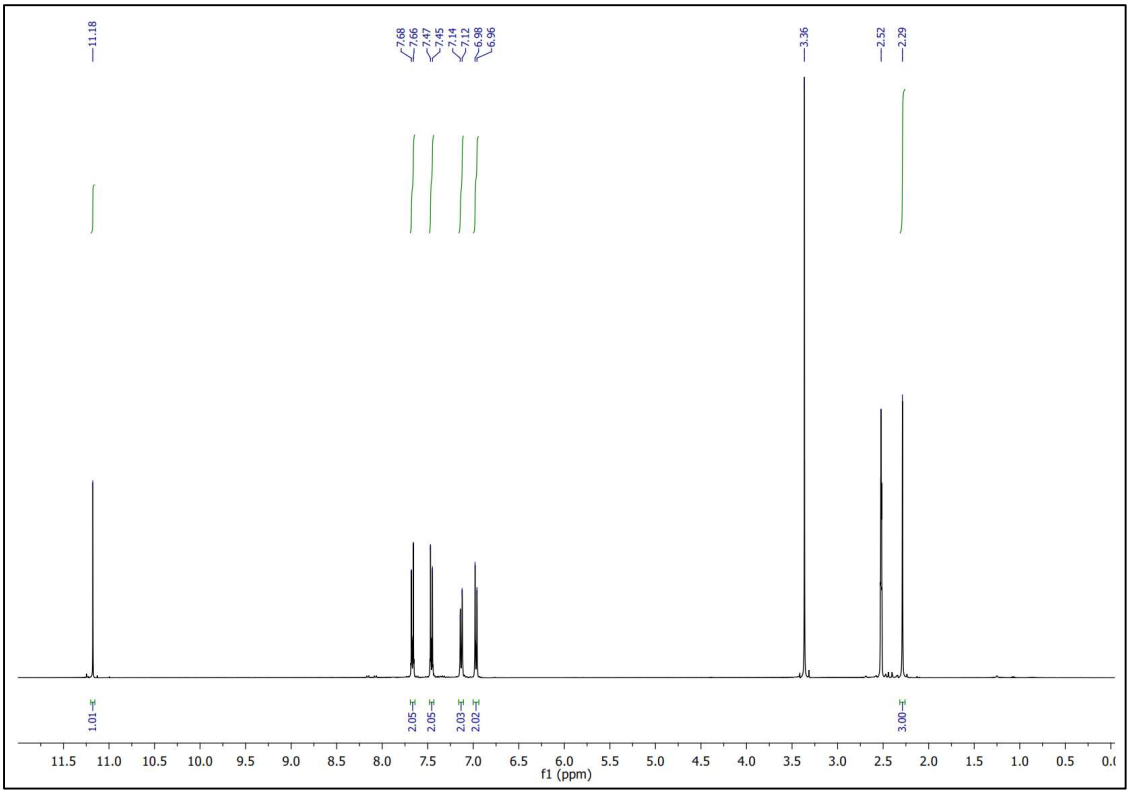


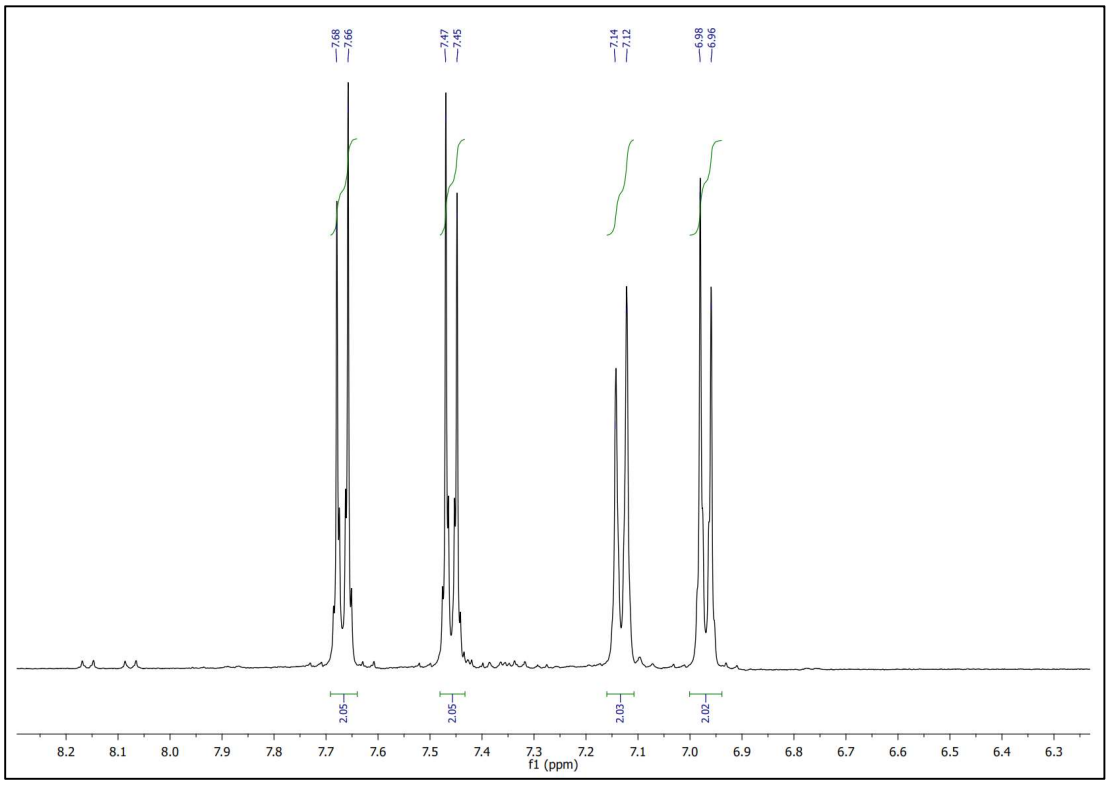


**Figure S23**. [1]HNMR spectra of 3

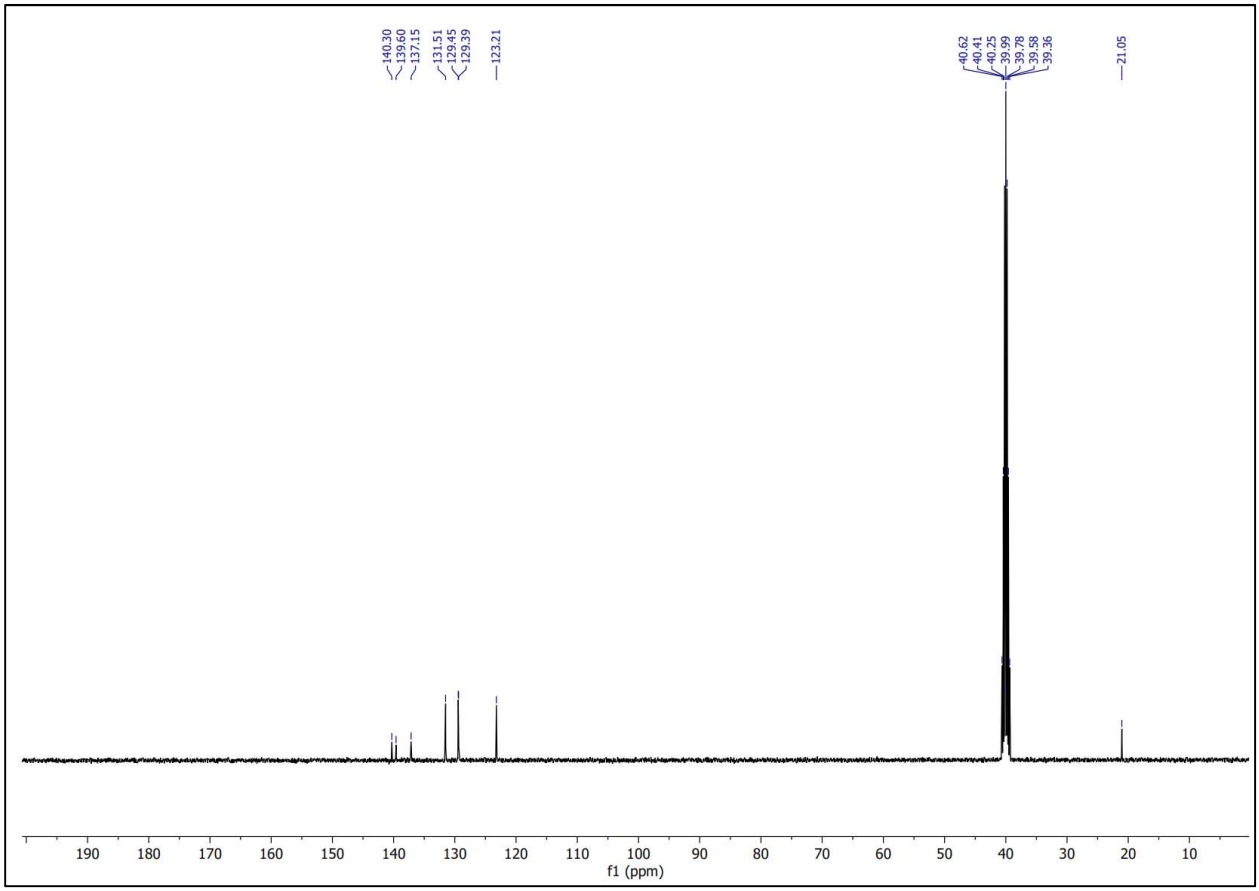


**Figure S24**. $^{13}$CNMR spectra of 3

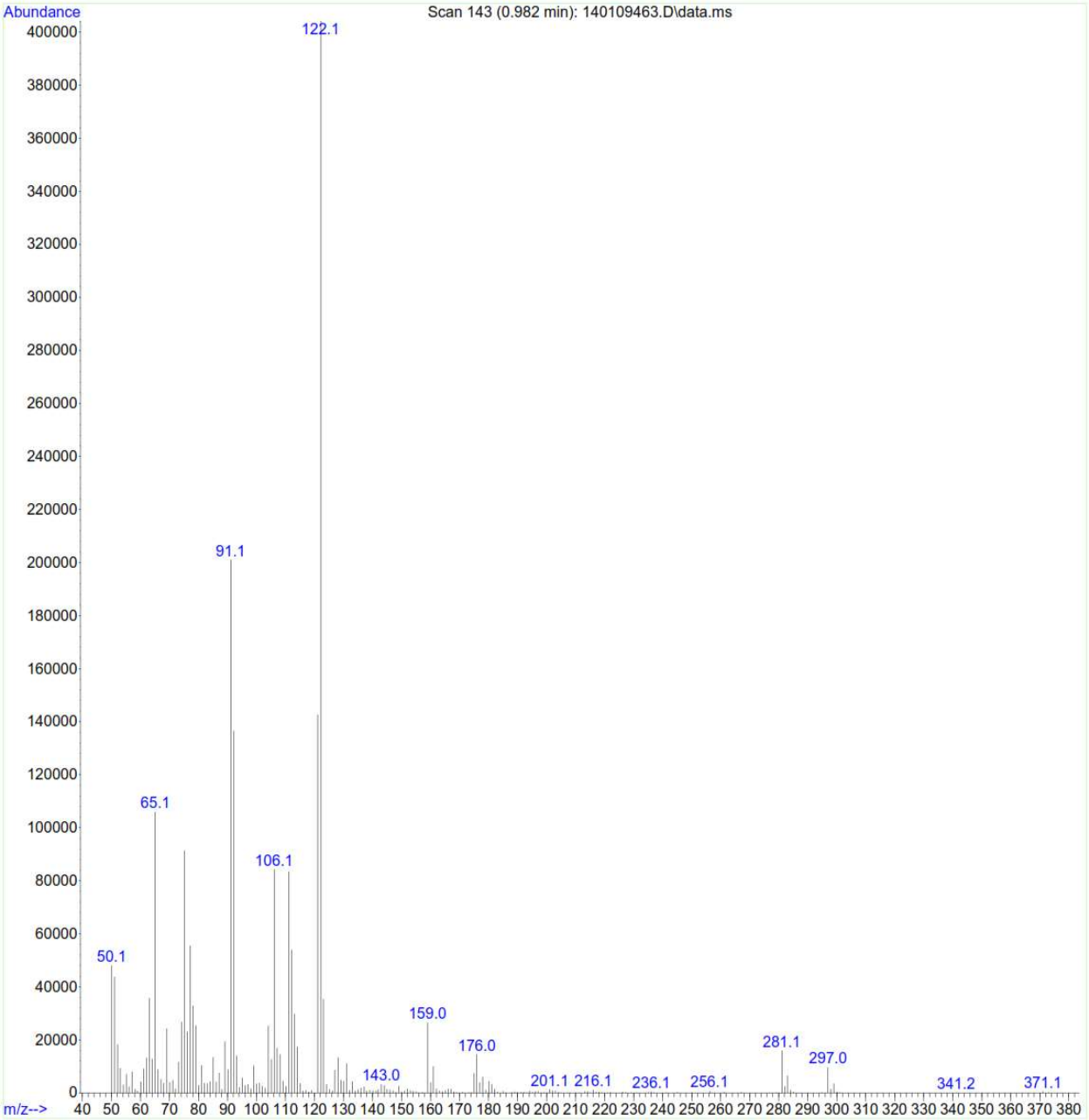


**Figure S25**. MS spectra of 3

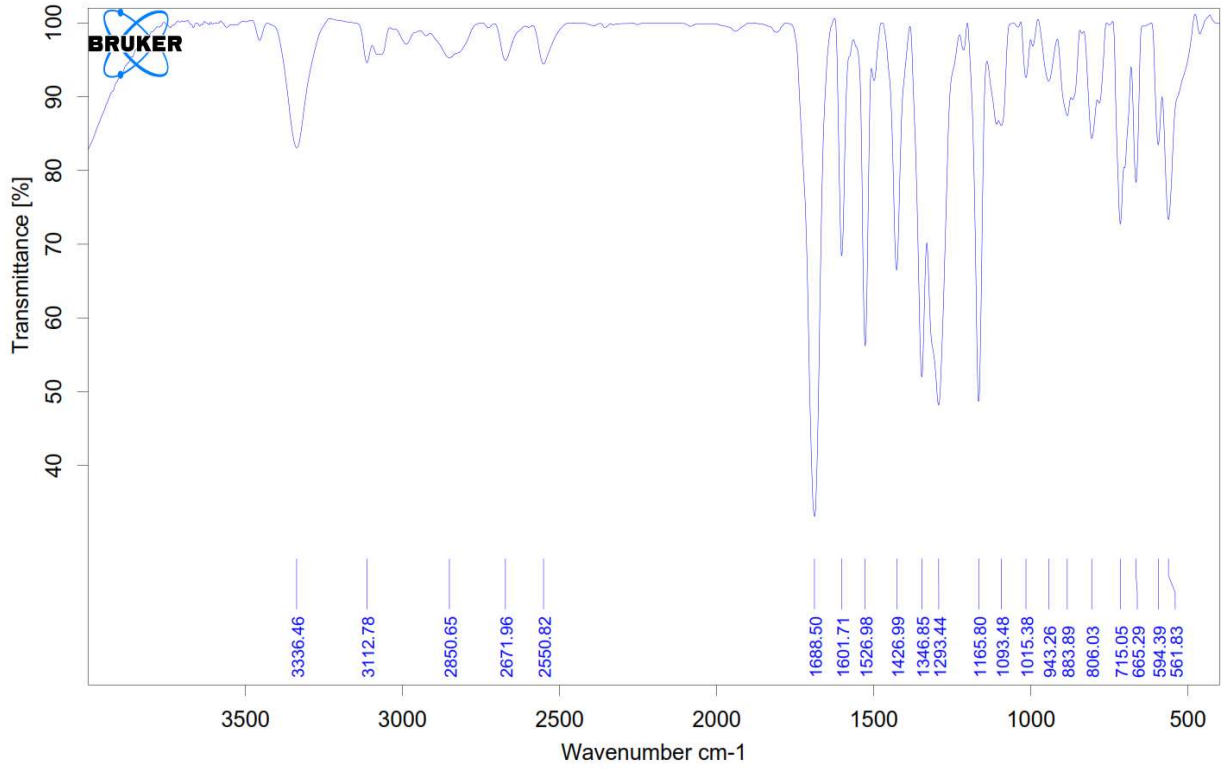


**Figure S26**. FTIR spectra of 4

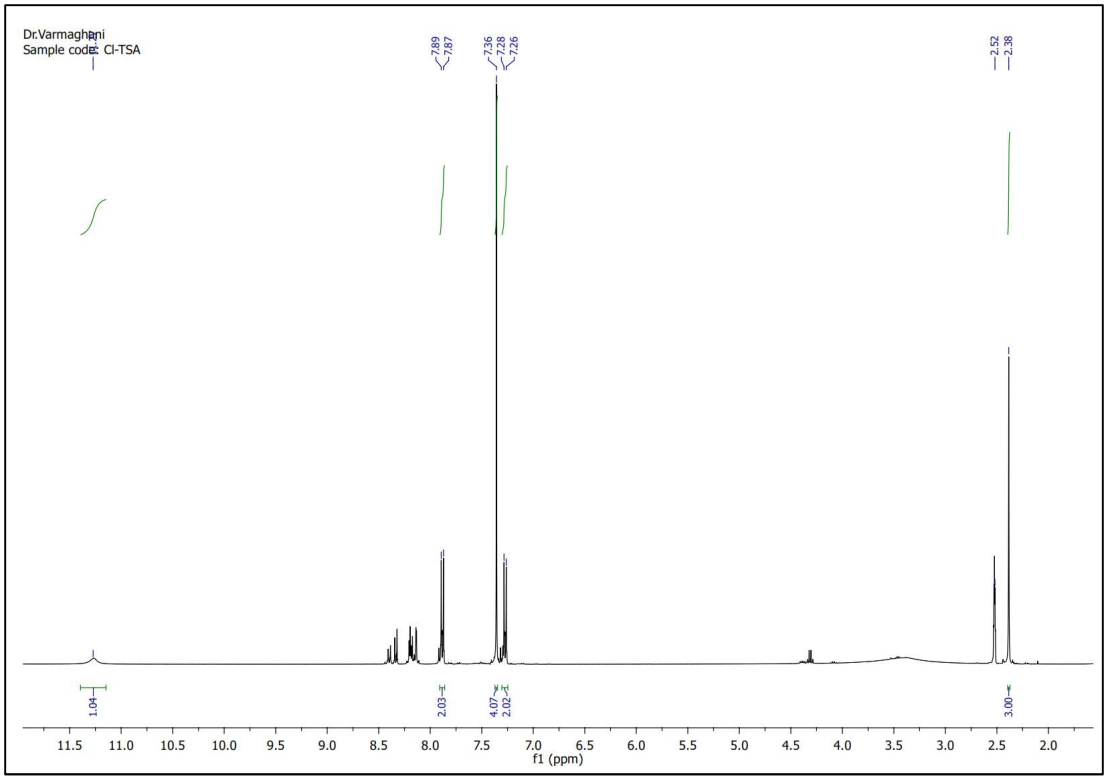


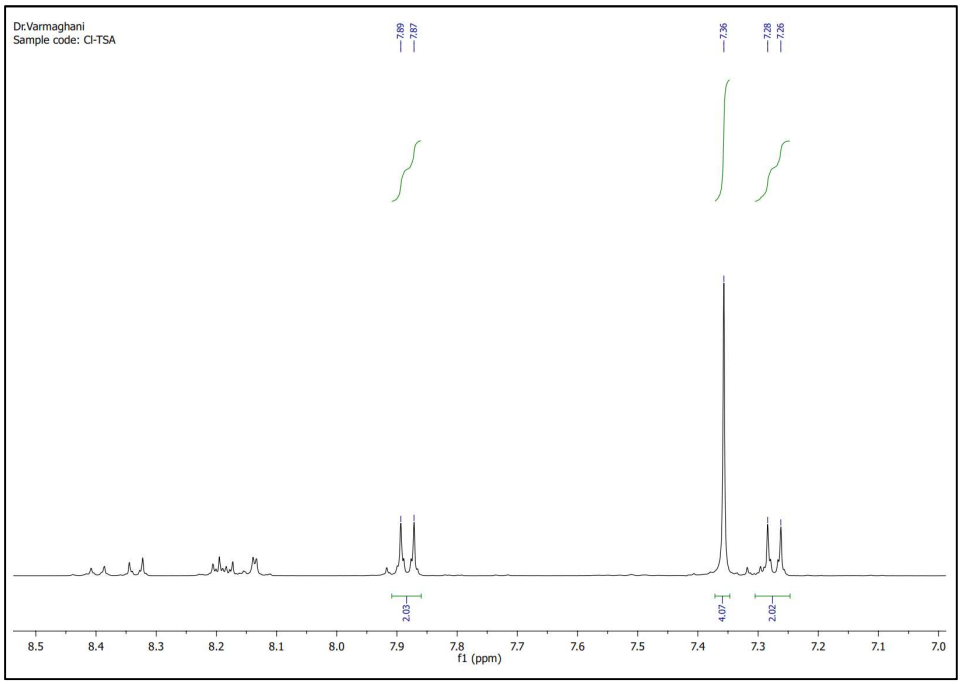


**Figure S27**. $^{1}$HNMR spectra of 4

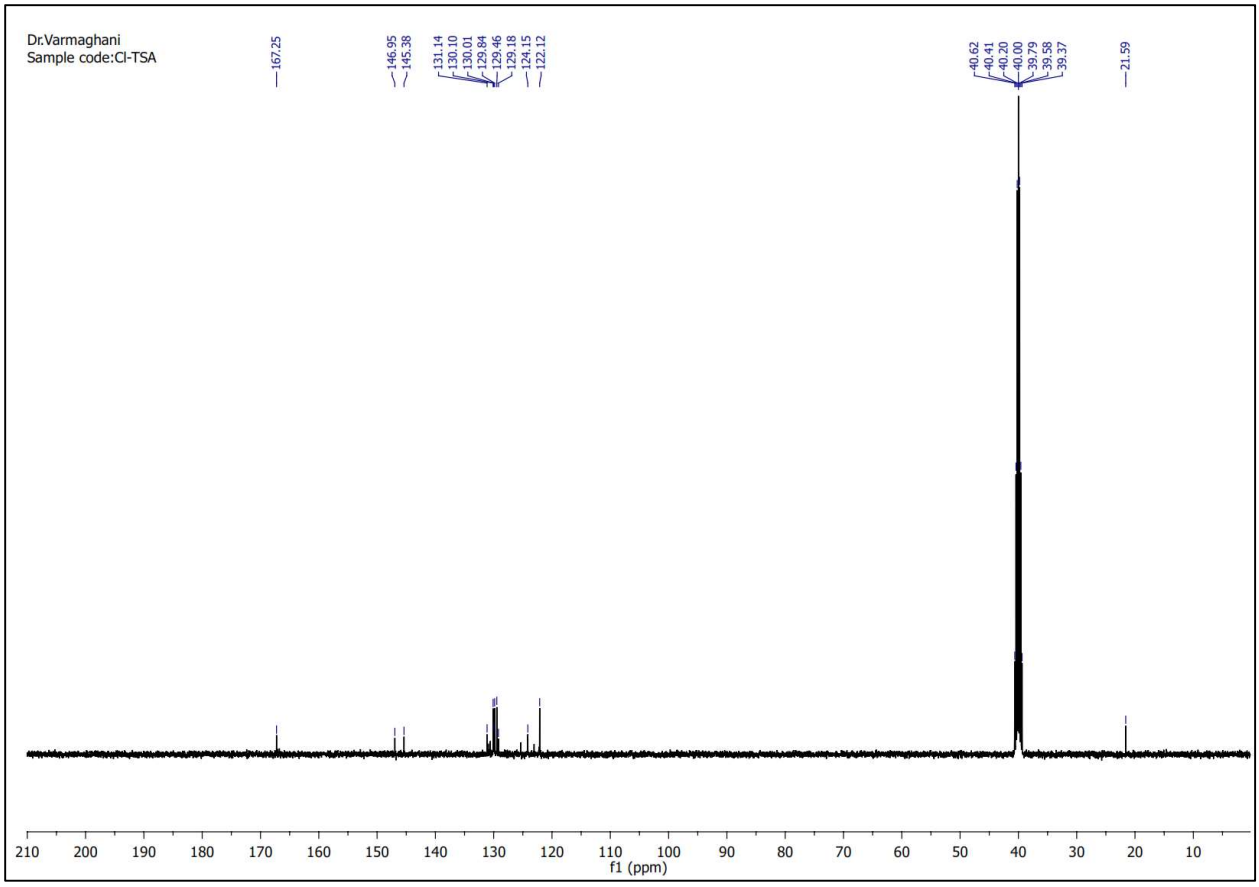


**Figure S28**. $^{13}$CNMR spectra of 4

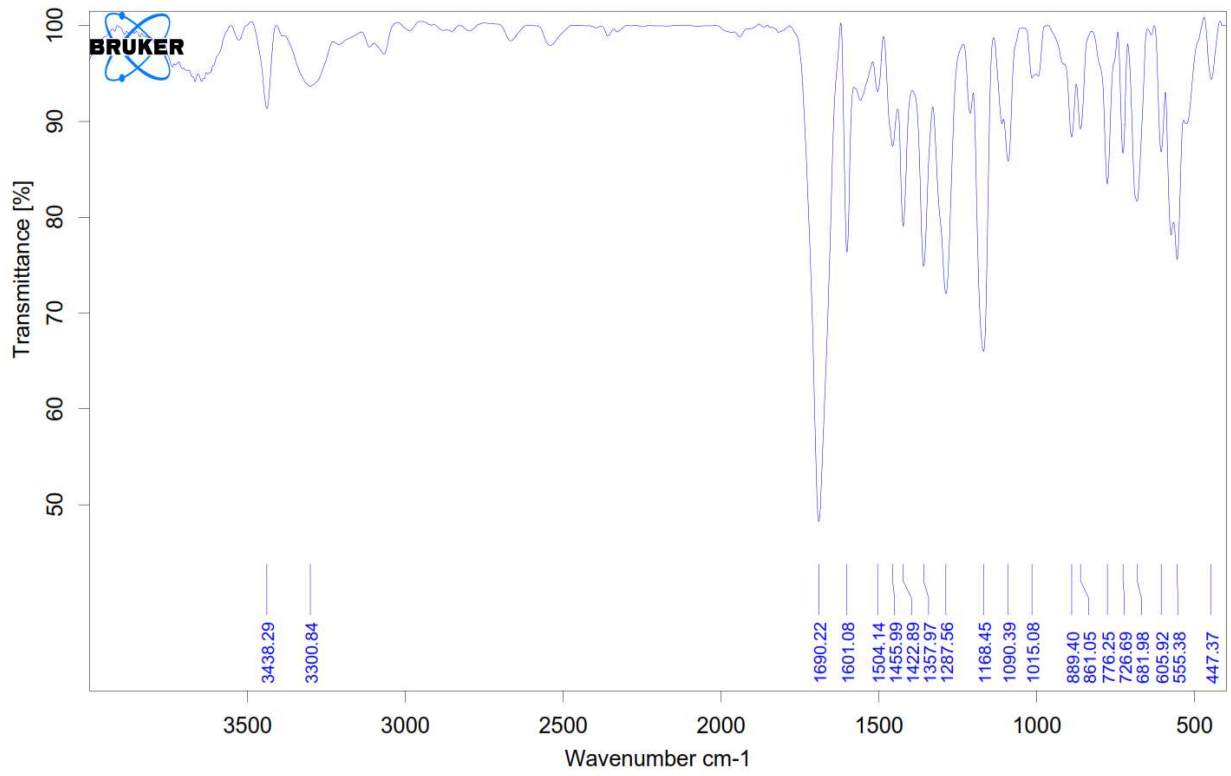


**Figure S29**. FTIR spectra of 5

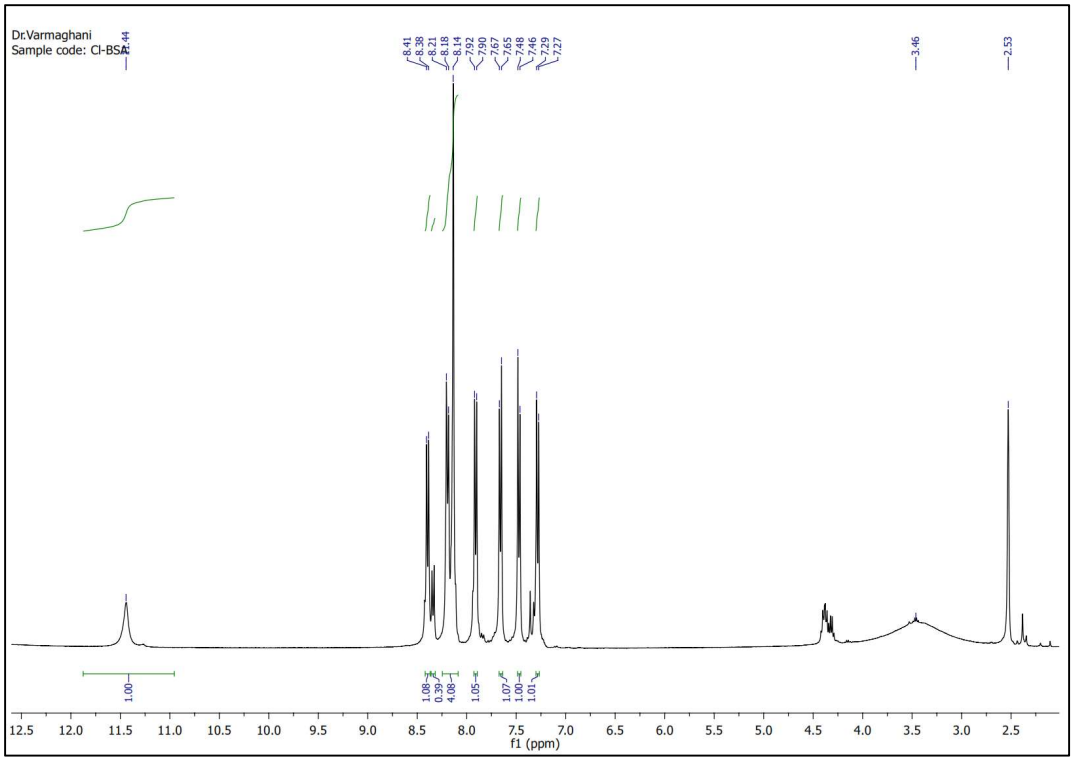


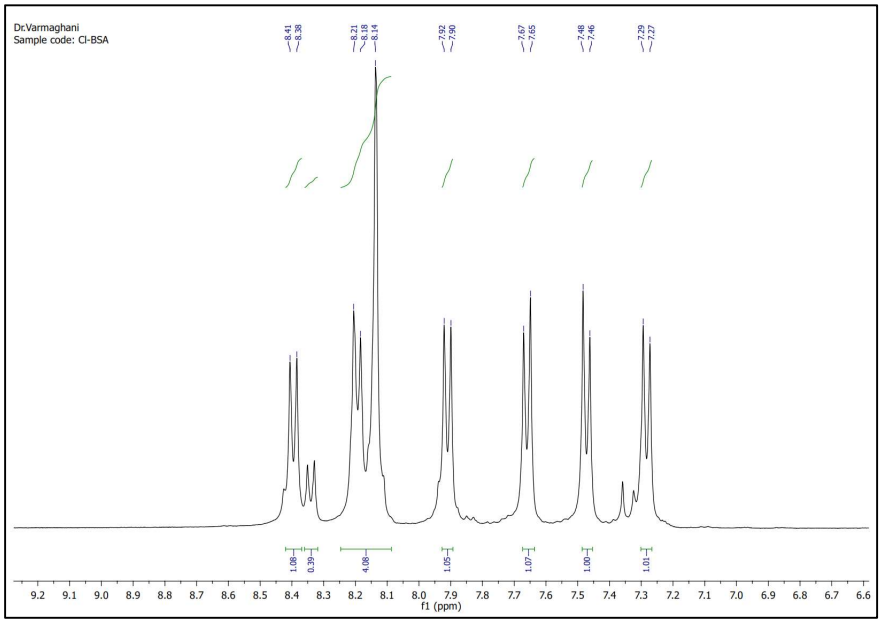


**Figure S30**. [1]HNMR spectra of 5

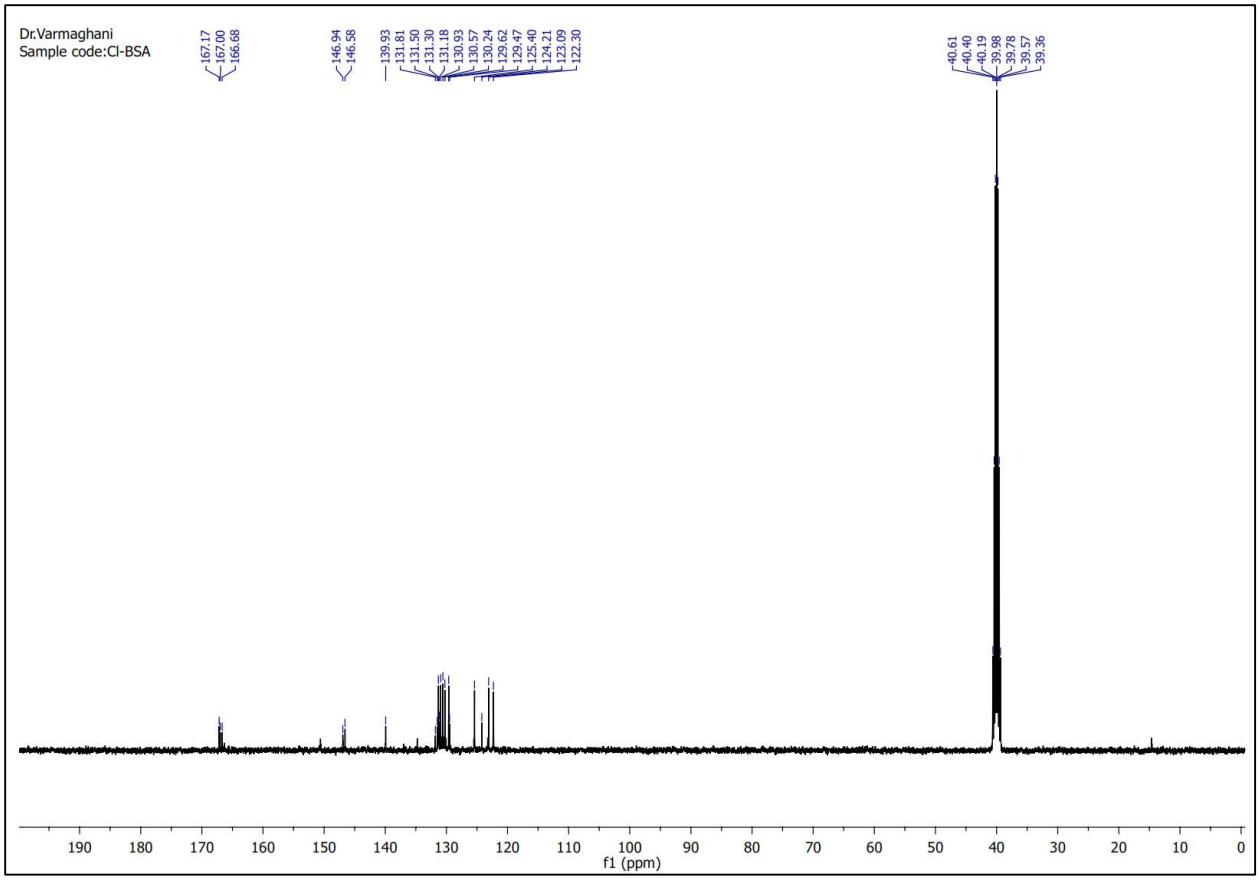


**Figure S31**. $^{13}$CNMR spectra of 5

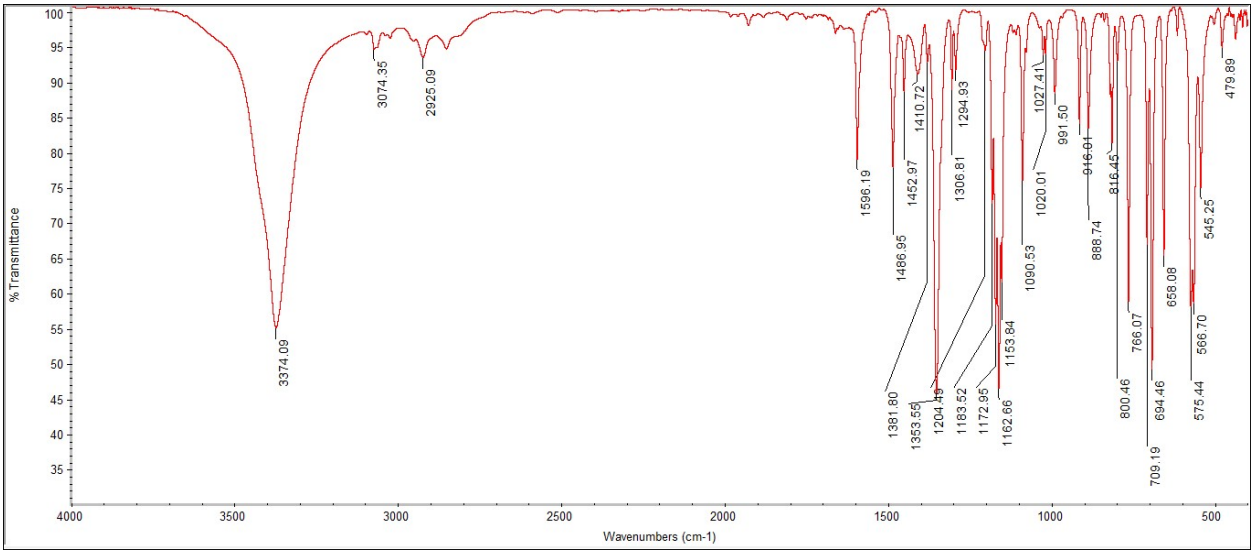


**Figure S32**. FTIR spectra of 6

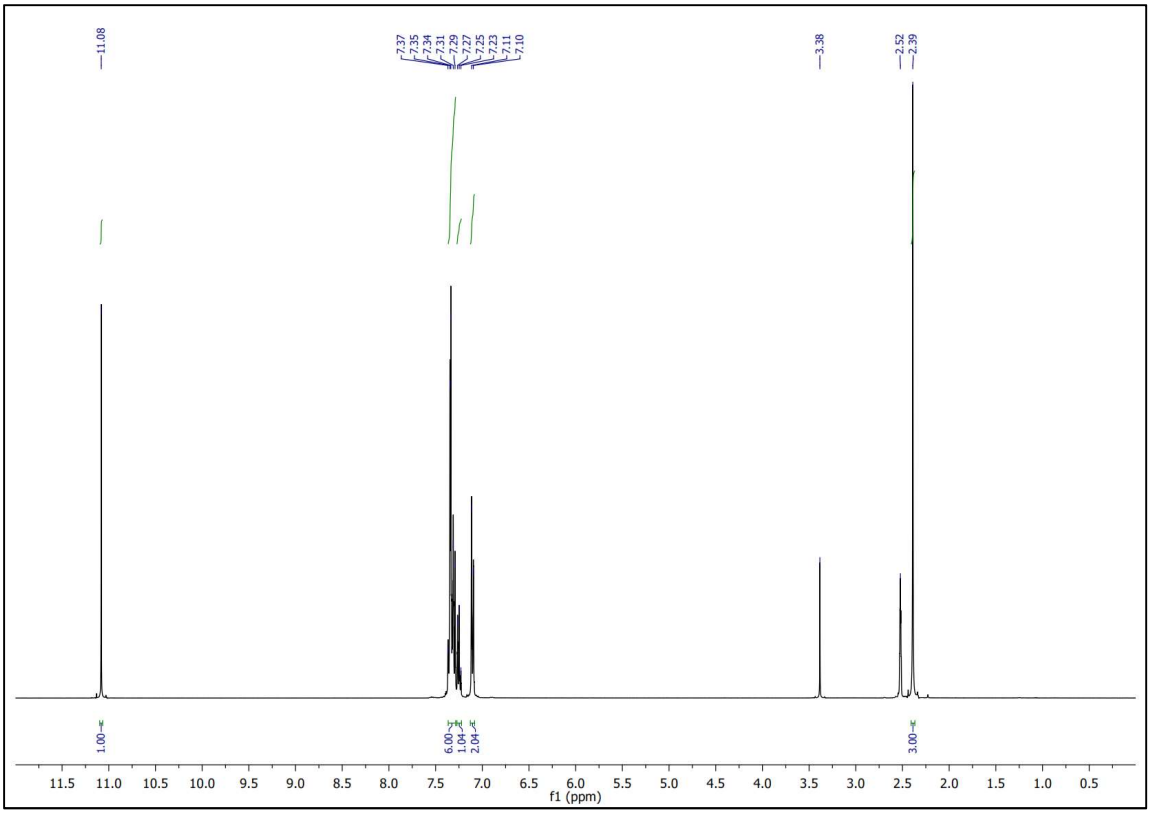


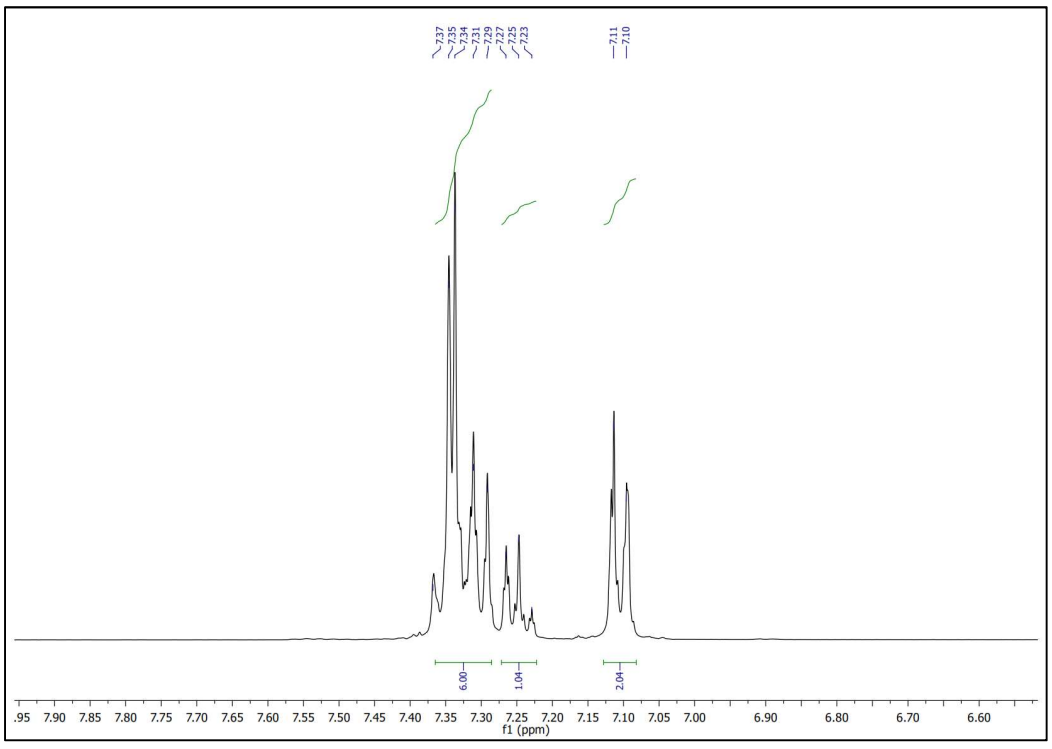


**Figure S33**. [1]HNMR spectra of 6

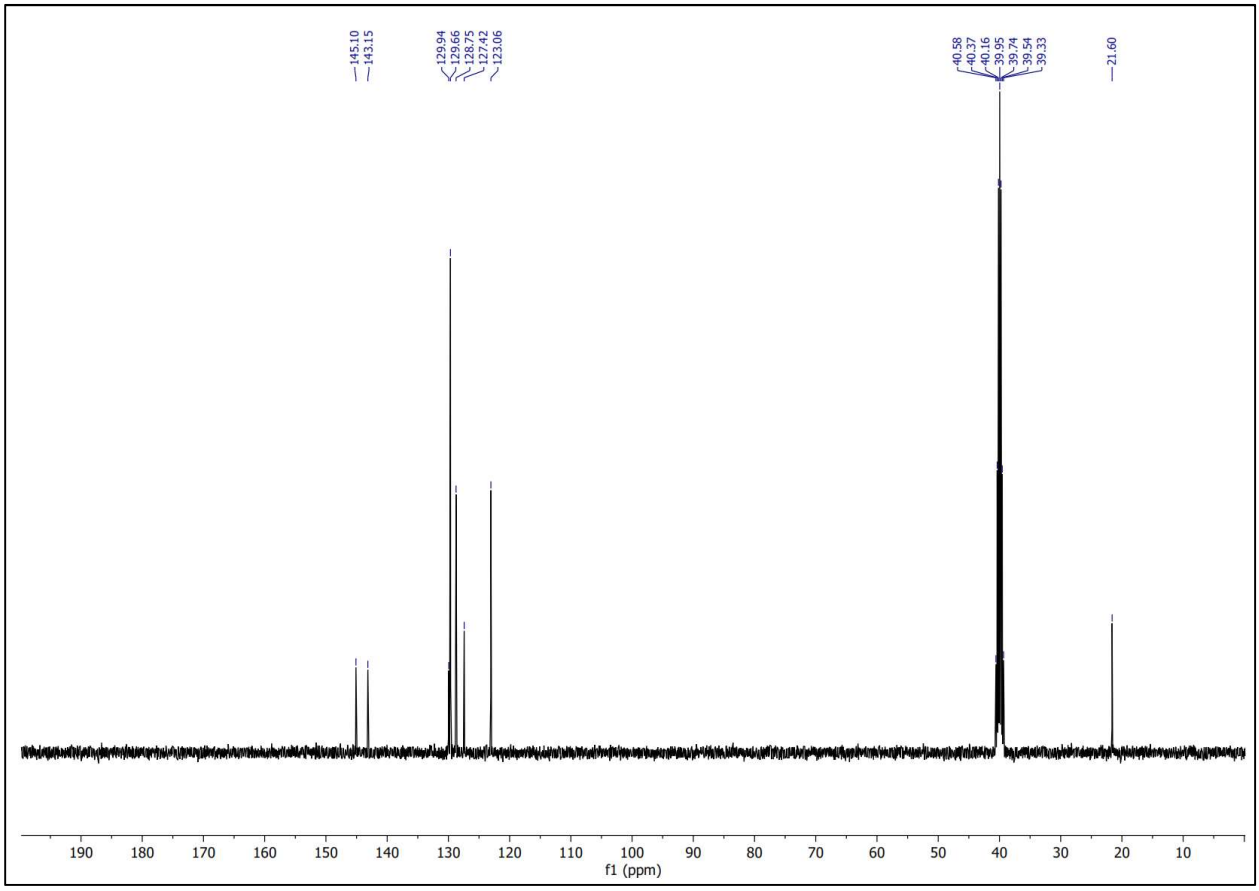


**Figure S34**. $^{13}$CNMR spectra of 6

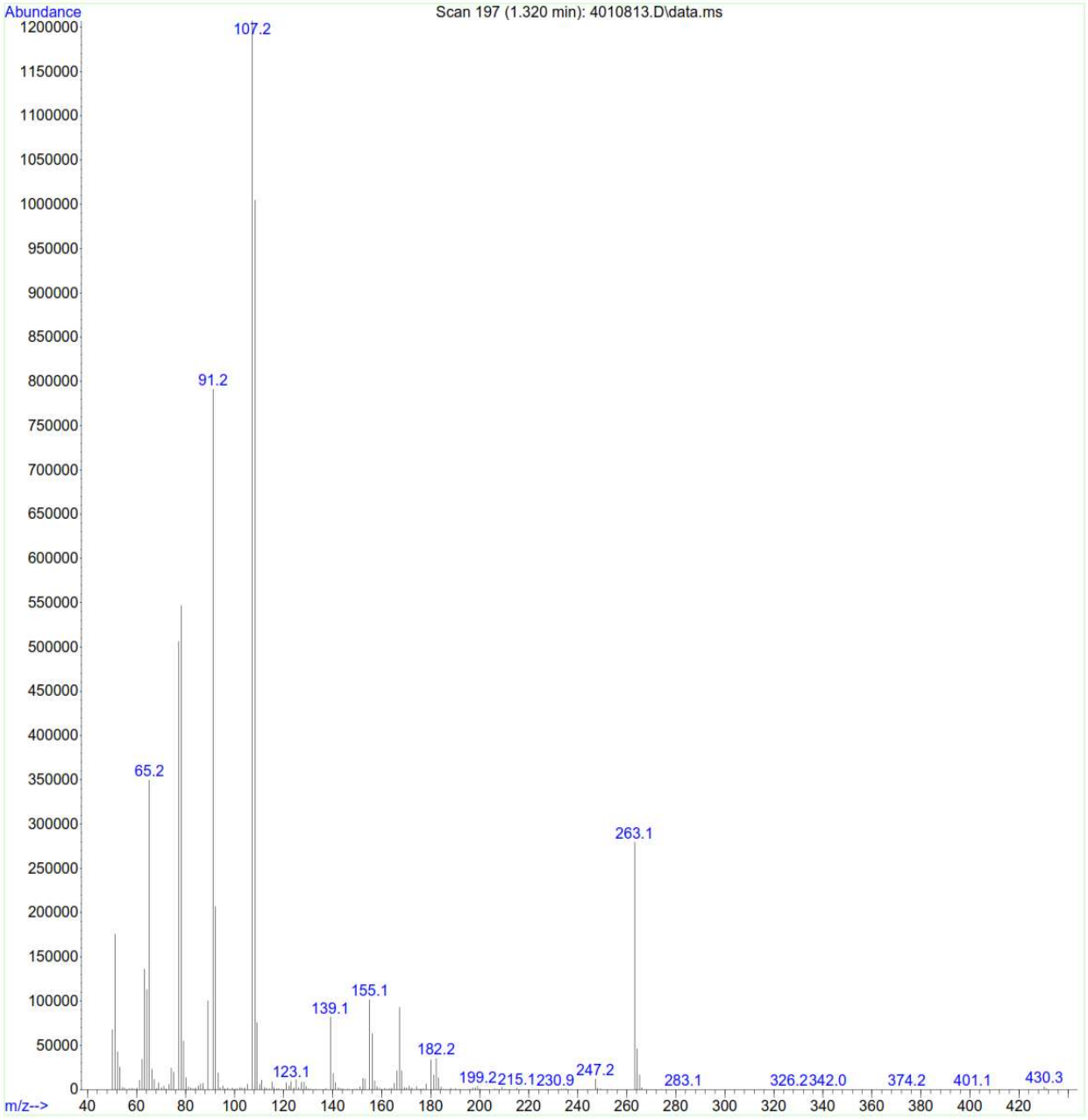


**Figure S35**. MS spectra of 6

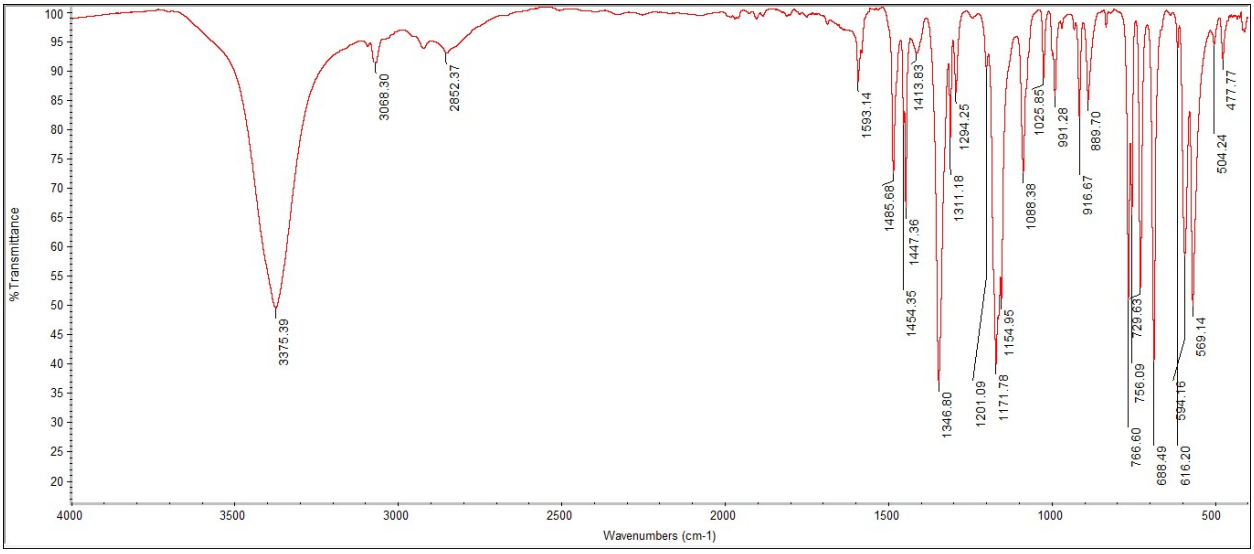


**Figure S36**. FTIR spectra of 7

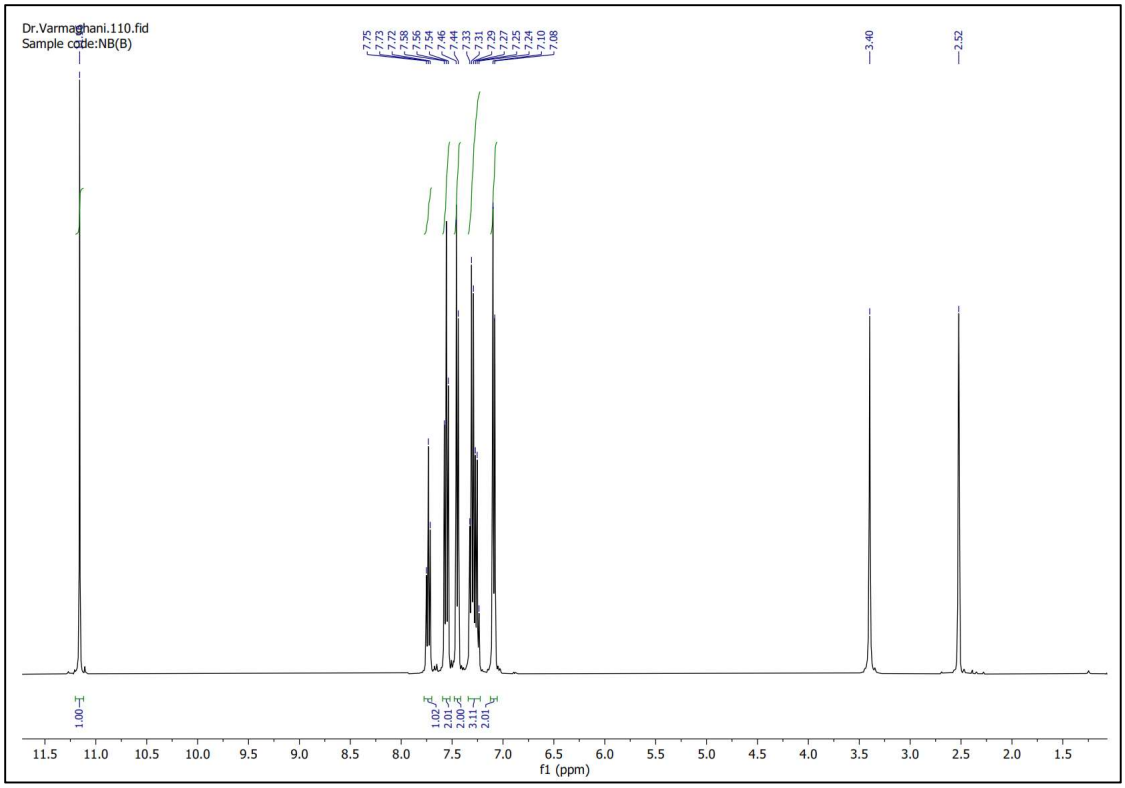


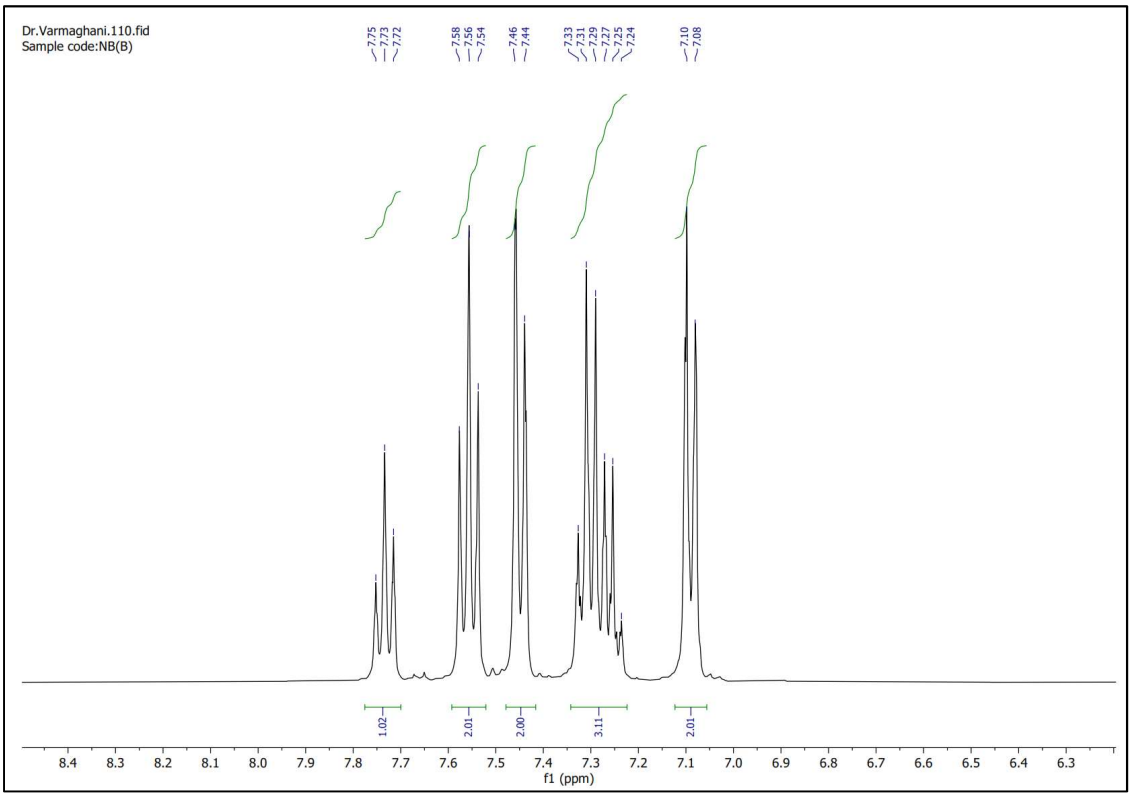


**Figure S37**. [1]HNMR spectra of 7

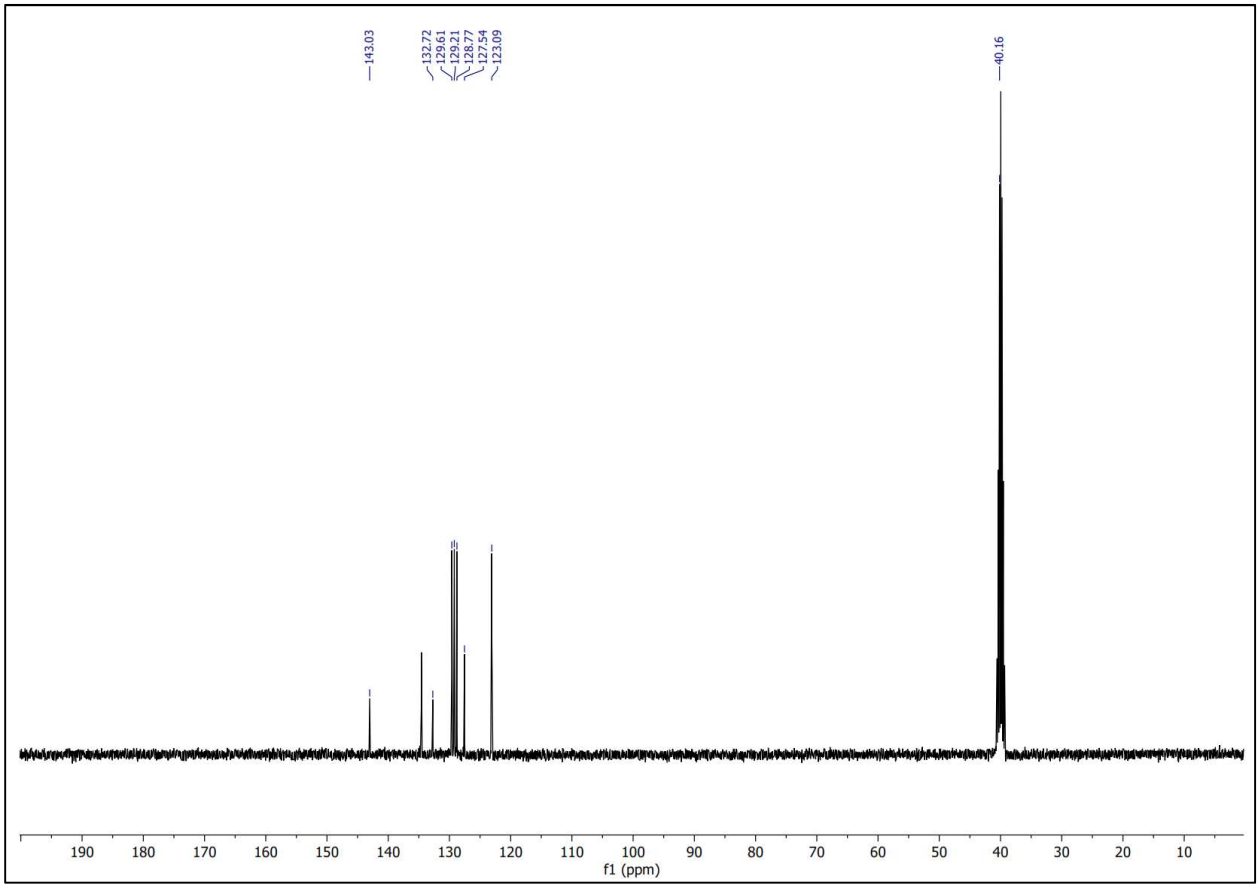


**Figure S38**. $^{13}$CNMR spectra of 7

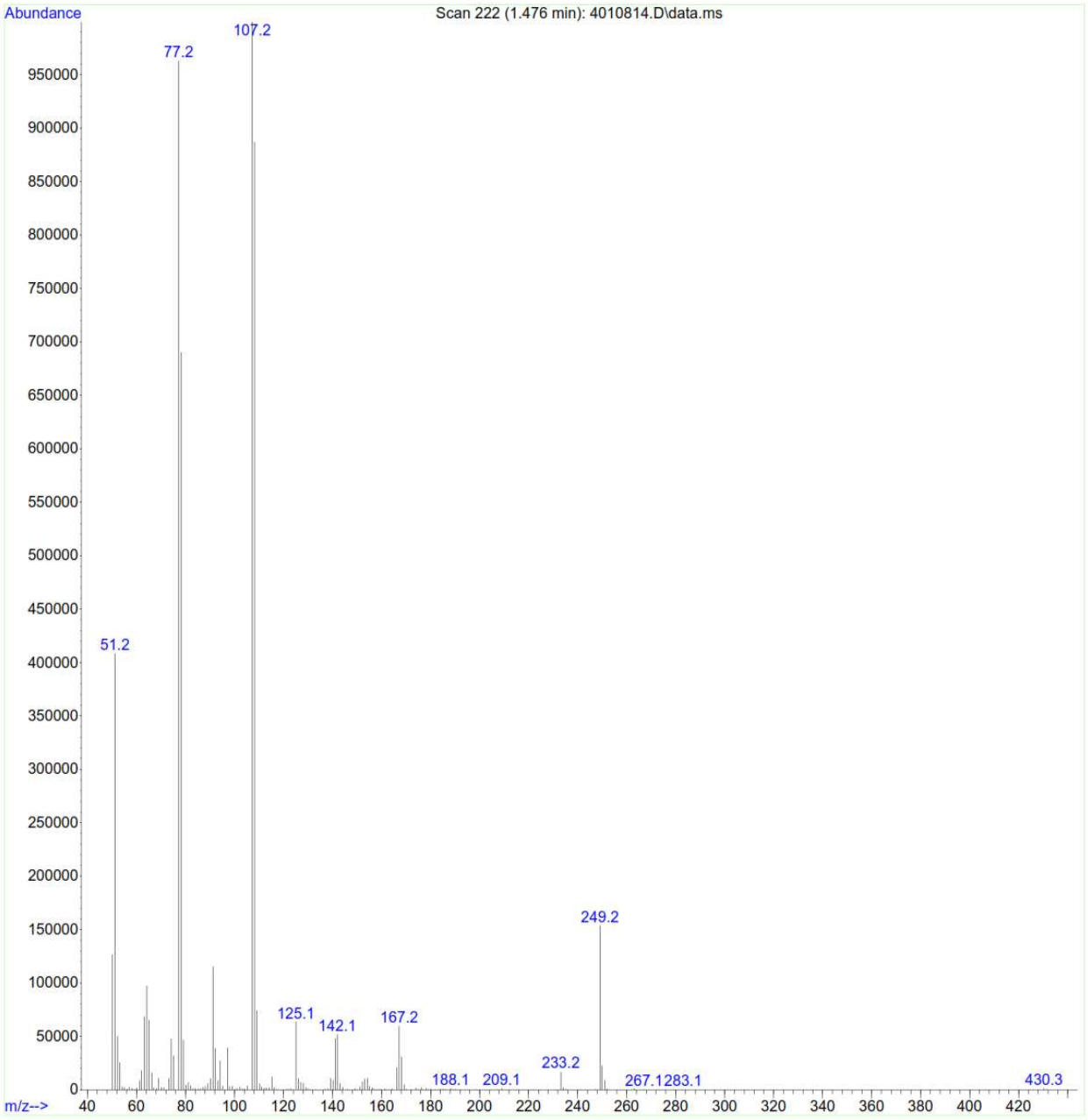


**Figure S39**. MS spectra of 7

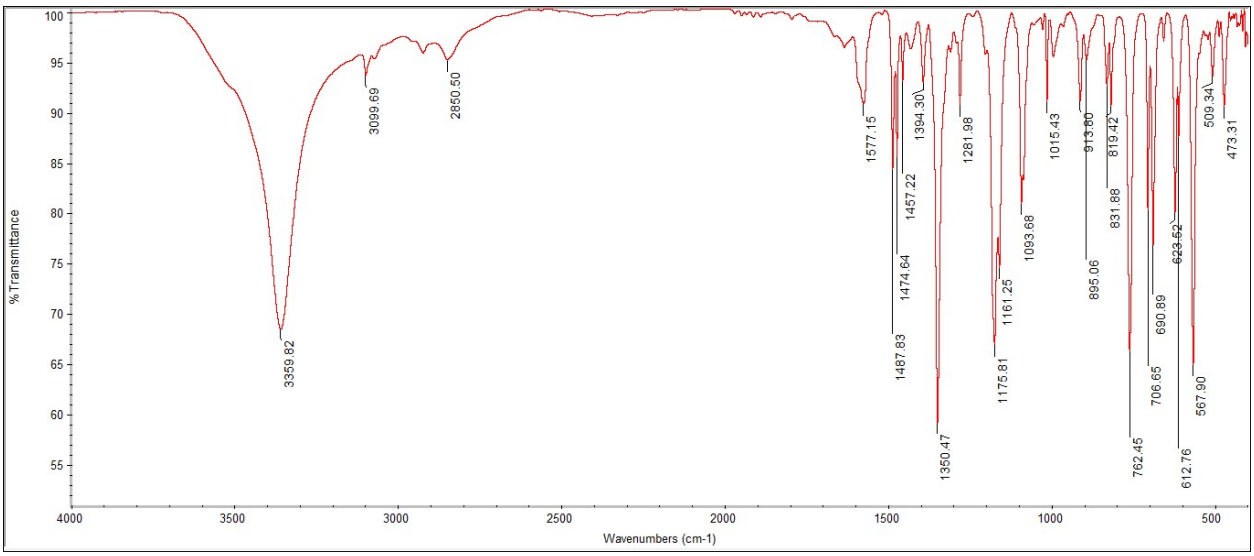


**Figure S40.** FTIR spectra of 8

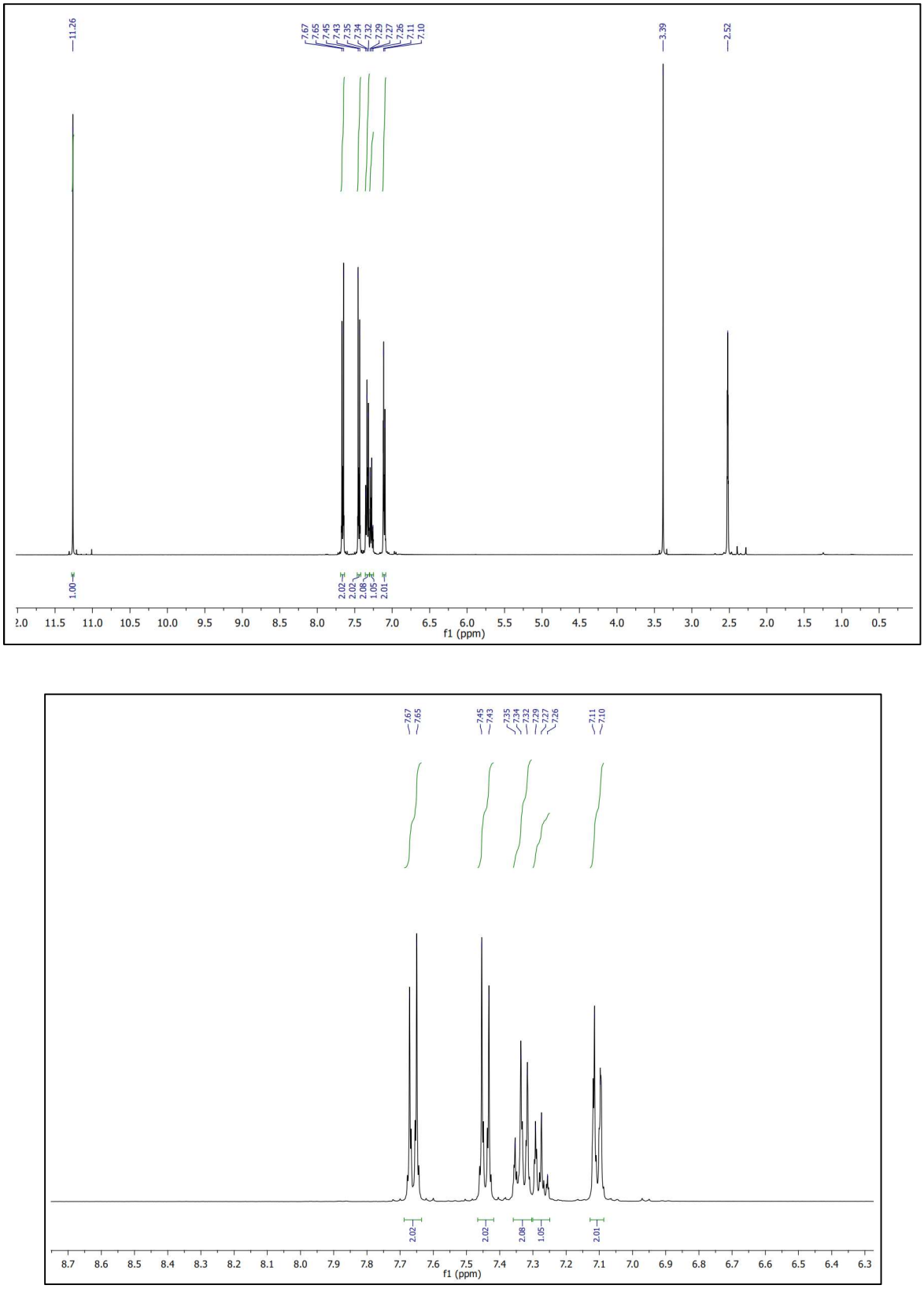


**Figure S41.** [1]HNMR spectra of 8

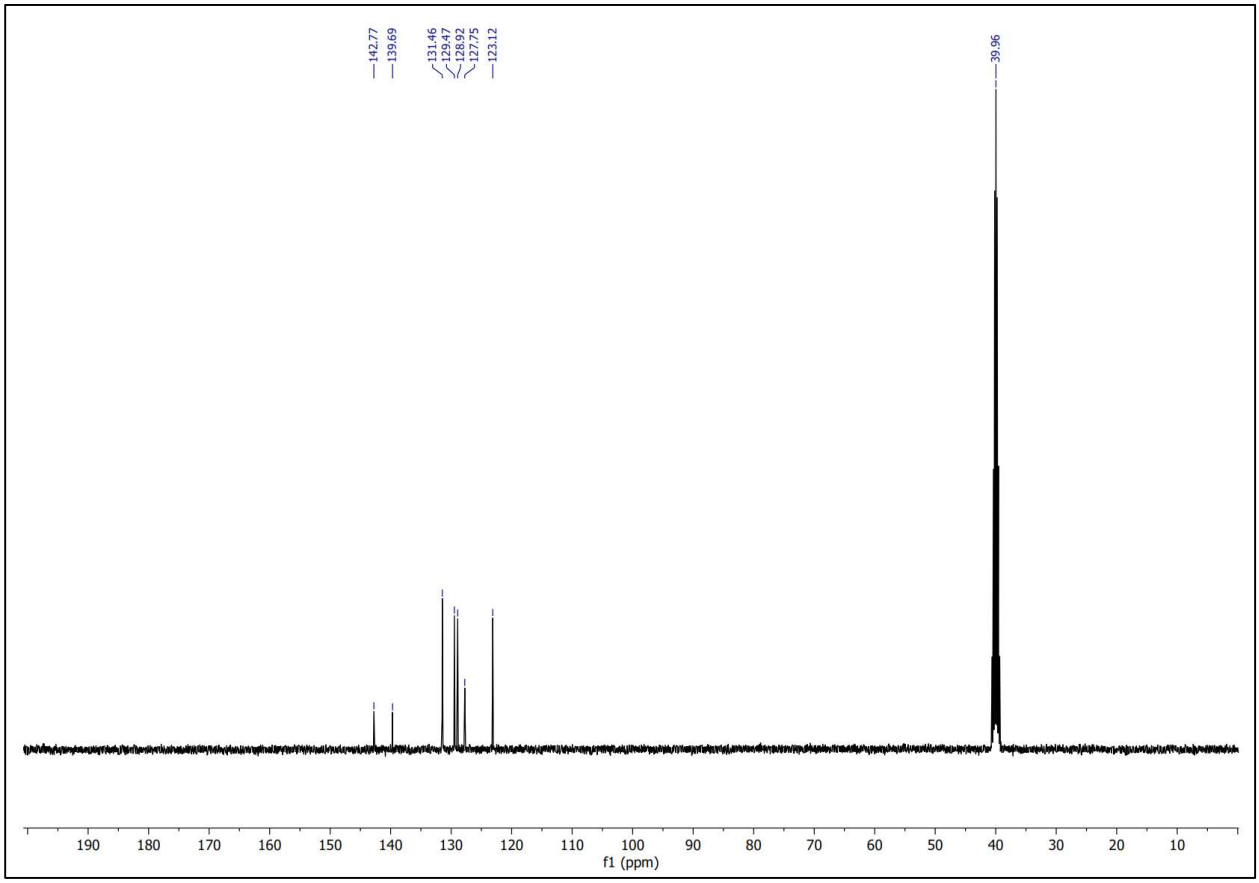


**Figure S42**. $^{13}$CNMR spectra of 8

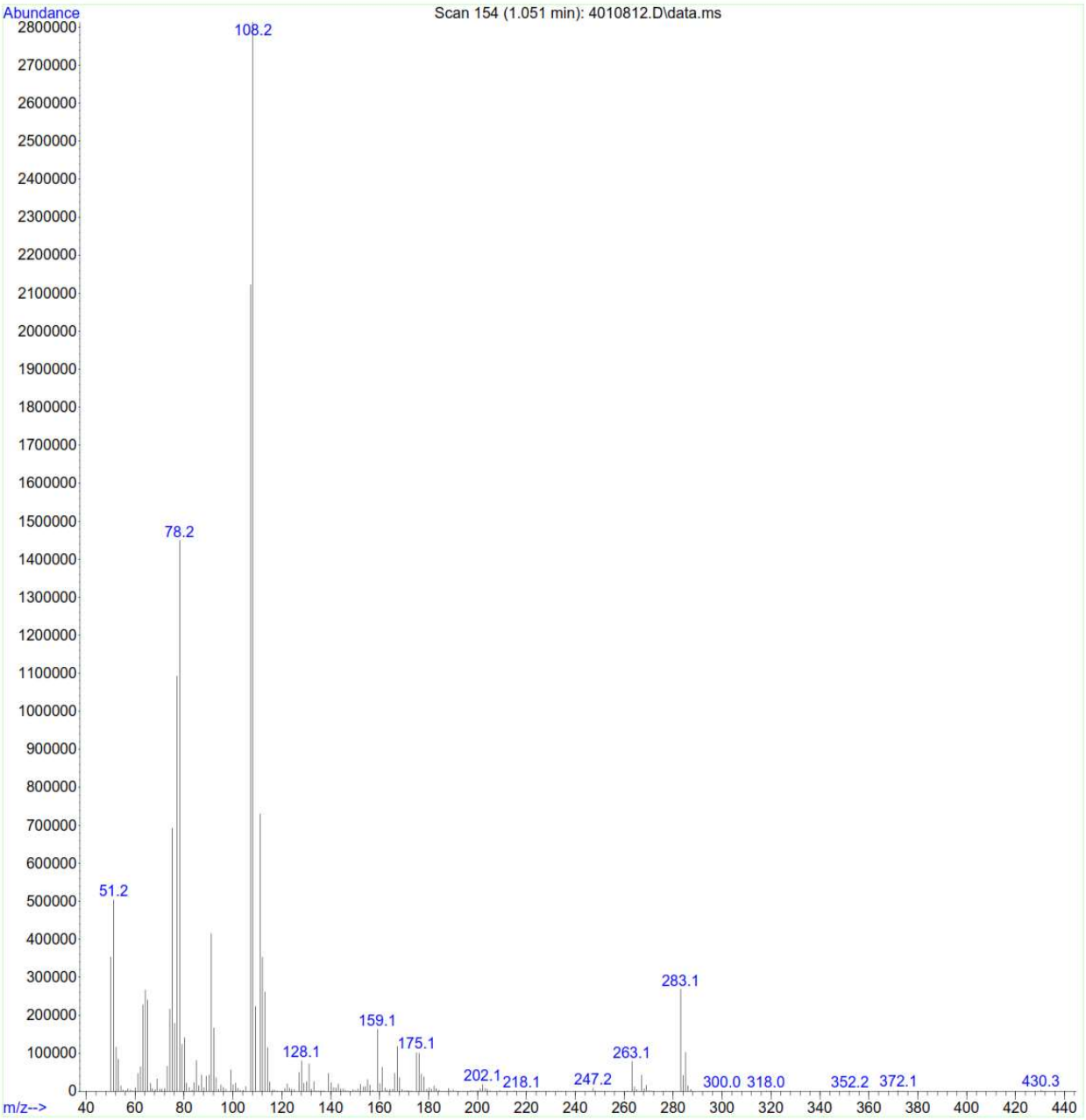


**Figure S43**. MS spectra of 8

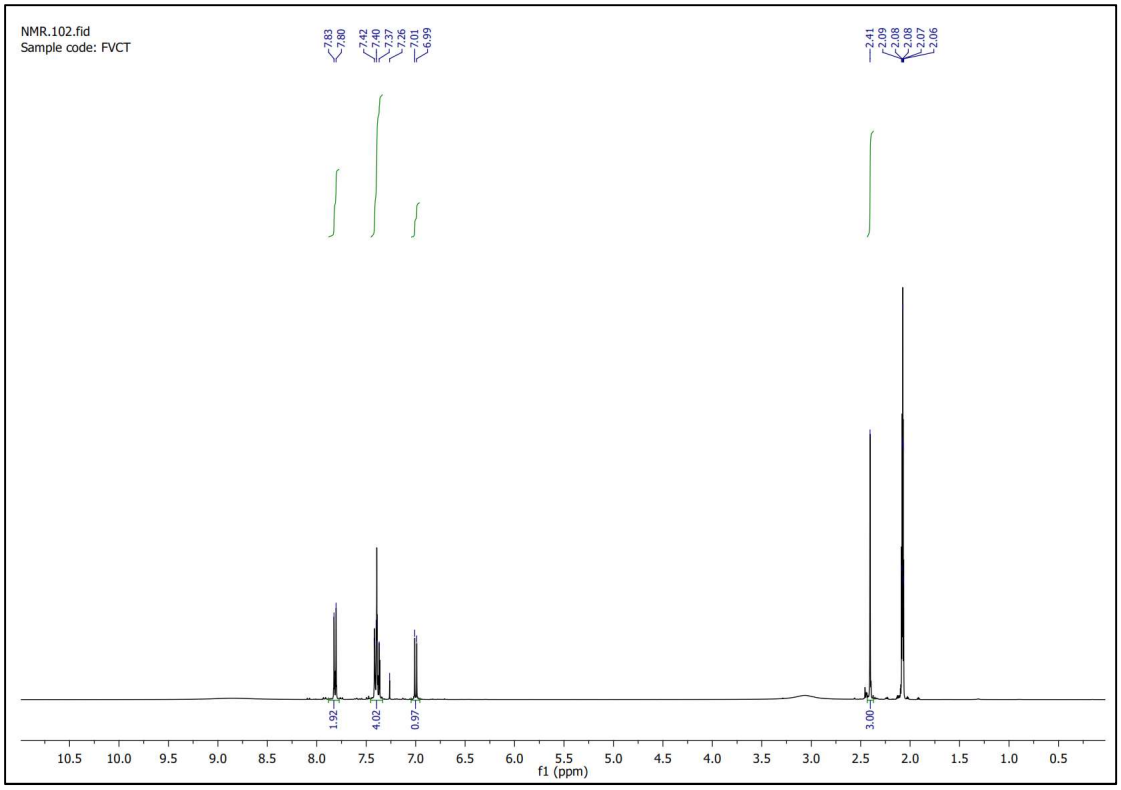


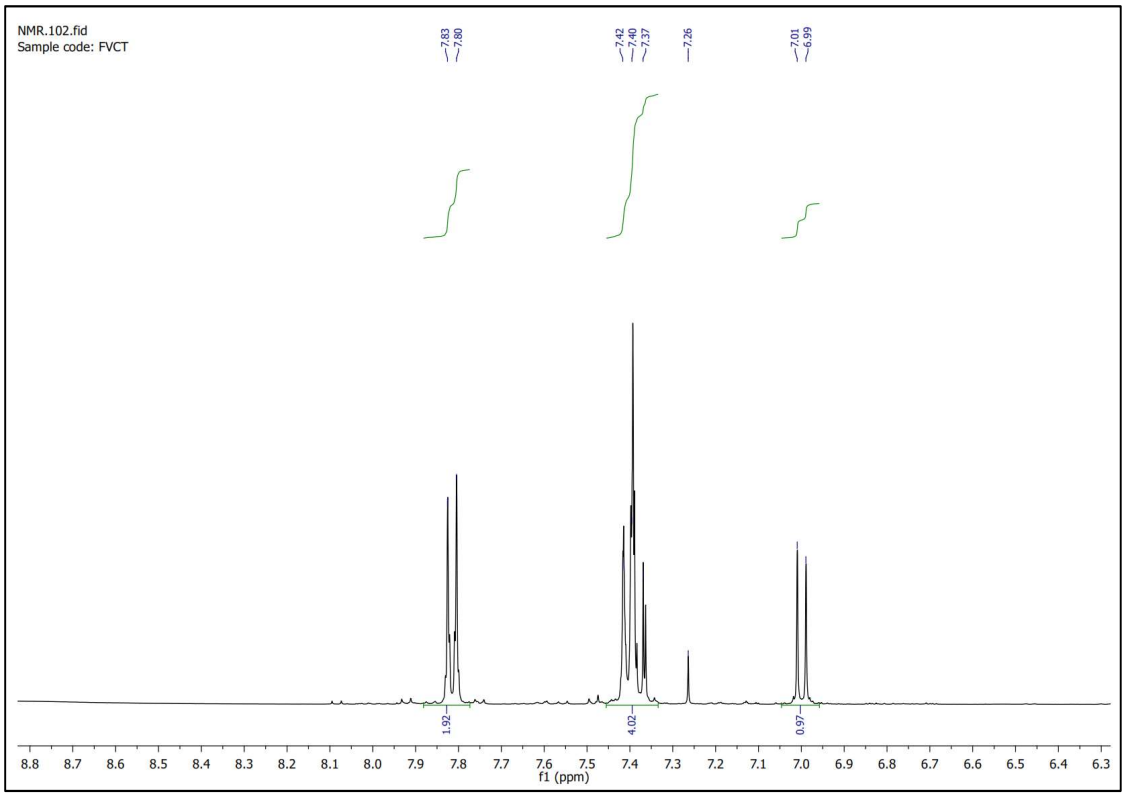


**Figure S44**. [1]HNMR spectra of 9

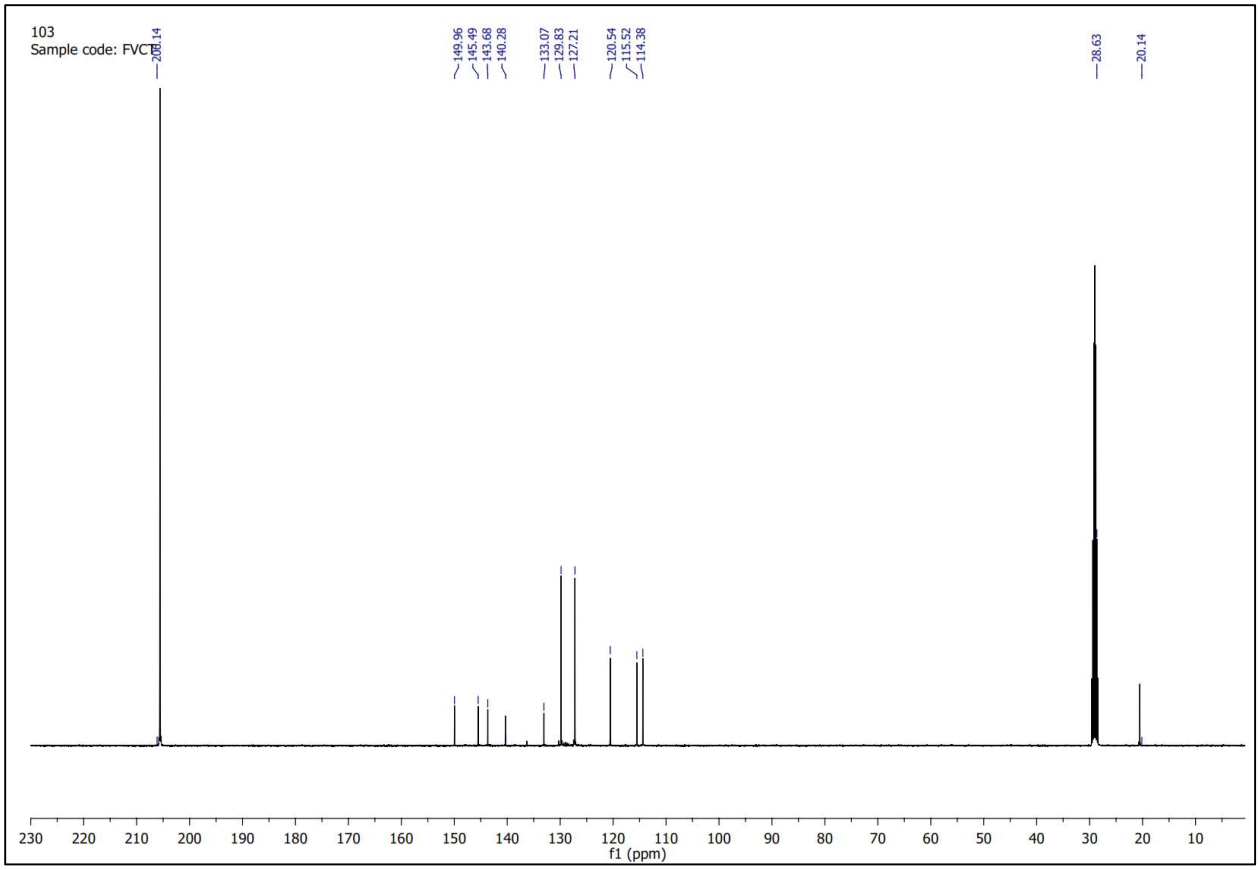


**Figure S45**. $^{13}$CNMR spectra of 9